POLITECNICO DI MILANO

SCHOOL OF CIVIL, ENVIRONMENTAL AND LAND MANAGEMENT ENGINEERING

MASTER OF SCIENCE IN CIVIL ENGINEERING FOR RISK MITIGATION

A WebGIS to show the Impact of the Grand Ethiopian Renaissance Dam on Agriculture in Egypt

Supervisor: Professor Daniela Carrion

Master Thesis By: Sherif Kheder

Academic year 2019-2020

Table of Contents

Table of Figures

Acknowledgements

I would like to thank my supervisor, Professor Daniela Carrion for her effort, patience, guidance, and support, without her effort, this thesis cannot be completed in this organized way. She was always available for my questions and to guide me on the right way to complete this thesis.

I would like to thank my friends Fadel and Lucia who gave me support to continue working to finish this thesis and they helped me with their valuable advices.

I would like to thank my family and my mother who were always helping me and supporting me from the beginning of my life.

Abstract (English)

Ethiopia has begun developing their significant hydropower potential with the construction of the Grand Ethiopian Renaissance Dam (GERD) on the Blue Nile River to facilitate local and regional growth. The GERD, located just upstream of the border with Sudan, is the first dam ever to be constructed directly on the main stem of the Blue Nile and will become the largest dam in Africa. The dam filling stage will have clear implications on downstream flows in Sudan and Egypt, complicated by evaporative losses, climate variability, and climate change. In this thesis, remote sensing imagery has been used in order to measure the impact of GERD on downstream area. A WebGIS application has been implemented to assess the effects of the dam on agriculture in Egypt specially Delta region, which is the last region before Nile River mouth. The application is calculating Enhanced Vegetation Index (EVI) for different regions downstream during past 20 years. Also, the developed application has a dynamic shareable interface that can be used either by experts or non-experts. On the other hand, the water resources and agricultural characteristics of Delta region are defined then, various analysis, using remote sensing, evaluated the vegetation level over Delta Region during last 20 years. The results show that the vegetation level in the middle of the Delta has minor changes. While, in the East and West of the Delta the vegetation level has incrementally increased to the double over the last 20 years. This increase is due to the reclamation of desert depending on underground water. Furthermore, the results show that the developed Web-based platform could promote a more comprehensive understanding of the problem, its outcomes, and the damage it could inflict on a given area.

Abstract (Italian)

L'Etiopia ha iniziato a sviluppare il proprio potenziale idroelettrico con la costruzione della Grand Ethiopian Renaissance Dam (GERD) sul fiume Nilo Azzurro per facilitare la crescita locale e regionale. La GERD, situata appena a monte del confine con il Sudan, è la prima diga mai costruita direttamente sul ramo principale del Nilo Azzurro e diventerà la più grande diga in Africa. La fase di riempimento della diga avrà chiare implicazioni sui flussi a valle in Sudan ed Egitto, complicata da perdite per evaporazione, variabilità climatica e cambiamenti climatici. In questa tesi, sono state utilizzate immagini telerilevate per misurare l'impatto della GERD sull'area a valle. E' stata inoltre realizzata un'applicazione WebGIS per valutare gli effetti della diga sull'agricoltura in Egitto, in particolare nella regione del Delta, l'ultima regione prima della foce del Nilo. L'applicazione permette di calcolare l'Enhanced Vegetation Index (EVI) per diverse regioni dell'Egitto per gli ultimi 20 anni. Inoltre, l'applicazione sviluppata ha un'interfaccia dinamica condivisibile che può essere utilizzata da esperti o non esperti. Nella tesi, vengono presentate le risorse idriche e le caratteristiche agricole della regione del Delta, varie analisi che utilizzano il telerilevamento hanno permesso di valutare il livello di vegetazione sulla regione del Delta negli ultimi 20 anni. I risultati mostrano che il livello della vegetazione della zona del Delta presenta lievi cambiamenti. Mentre, nell'est e nell'ovest del delta, il livello della vegetazione è aumentato gradualmente fino a raddoppiare negli ultimi 20 anni. Questo aumento è dovuto alla bonifica del deserto e allo sfruttamento delle acque sotterranee. Inoltre, i risultati mostrano che la piattaforma Web sviluppata potrebbe promuovere una comprensione più completa del problema, dei suoi esiti e del danno che potrebbe infliggere in una determinata area.

CHAPTER 1: INTRODUCTION

1.1 Introduction

Egypt is in Northeast Africa and it is a part of Sahara Desert which is one of the hottest and driest area in the world. There are two main sources of water in Egypt, Nile River which represent 90-95% of water supply and underground water which represent 5-10% of water supply. Nile River is North flowing river which has two major tributaries, The White Nile, and the Blue Nile. The White Nile is the headwaters and primary stream of the Nile itself. However, The Blue Nile is the source of most of the water, containing 80% of the water and silt. Ethiopia has begun developing their significant hydropower potential by the construction of the Grand Ethiopian Renaissance Dam (GERD) on the Blue Nile River to facilitate local and regional growth. The GERD located just upstream of the border with Sudan, it is the first dam ever to be constructed directly on the main stem of the Blue Nile and will become the largest dam in Africa. Although this has required substantial planning on Ethiopia's part, no policy dictating the reservoir filling rate strategy has been publicly issued. This filling stage will have clear implications on downstream flows in Sudan and Egypt. The annual Egypt share of Nile River could be reduced by 25% during the filling of GERD. Consequently, it is Expected that agriculture in Egypt will be affected due to the lack of Water. While Negotiation between Egypt, Ethiopia and Sudan did not lead to any agreement yet. Also, there is conflict of information between countries in dispute.

The focus of this thesis is measuring the impact of the Grand Ethiopian Renaissance Dam (GERD) on Egypt during the time period of Dam filling and how the agriculture in Egypt will be affected due to the reduction of Egypt's share from Nile River .Furthermore, it focuses on observing vegetation changes in Egypt during the last 20 years and reasons behind Vegetation level variations.

The goal of this thesis is to study the characteristics of the affected area in Egypt. Furthermore, create WebGIS tool to measure the impact of GERD on Egypt over the next years, while the filling time. The used tool needs to be easily modified to provide sustainable update of the recent changes of the situation. Also, it needs to be neutral to help solving information conflict between different parties. And, it is important to fulfill the requirement of easy sharing, reviewing, and modifying to be joint venture between stakeholders, users, and different organization.

CHAPTER 2: GERD and The Potential Impact on Egypt

2.1 Overview of Nile River water availability in Egypt

The Nile River is located at the northeast of Africa and its basin is considered as the longest on the world. Among it, several distinct hydroclimatic regions are found. The Equatorial Lake Plateau in the south, the Bahr el-Ghazal in the center, and the Ethiopian Highlands in the east are the main watersheds from where the Nile receives its flows. From the confluence of Atbara River north of Khartoum to the Mediterranean Sea, the Nile receives no effective inflow. (NBI, 2012).

For thousands of years, the Nile has been an important water resource on the area, due to this, almost all the cultural and historical sites of ancient Egypt are found along its riverbanks. Nowadays, the Nile serves to 11 countries: Tanzania, Uganda, Rwanda, Burundi, the Democratic Republic of the Congo, Kenya, Ethiopia, Eritrea, South Sudan, Sudan, and Egypt (Figure 2.1) (Tayie, 2018). In Egypt, the 97% of water resources come from the Nile, it means a direct dependency between the river and the survival of the country.

Figure 2.1 Nile basin with the forthcoming GERD (modified from World Wildlife Fund 2007)

The region in South Sudan is fed by interconnected lakes in Tanzania, Kenya, and Uganda. This region presents many swamps and lagoons that show a regulating effect by growing considerably during times of high inflow, allowing for increased evaporation, and releasing at a more moderate rate (Sutcliffe & Parks, 1987). In Sudan, the Blue Nile continues flowing northwest is joined most remarkably with the Dinder-Rahad River, together flowing through the Gezira Scheme—one of the largest irrigation projects in the world—and finally converges with the White Nile. From Khartoum, the main Nile flows in direction to north, crossing the entering Sahara Desert, and approximately 300 km north of Khartoum is joined from the east by the Atbara River. The Nile later enters Lake Nasser on the Sudanese-Egyptian border, this lake was created by the High Aswan Dam, and subsequently flows through Egypt to the Mediterranean Sea.

the Nile river is the Longest river in the world, it has a very short amount of water in comparison to the other long rivers in the world. Figure 2.2 shows the histogram of the longest rivers in the world with the water shared percentage. the water share in the Nile River is almost disappeared in comparison to the other long rivers like Amazon River which share about 20% of the global fresh water. As a result, there is a problem of water scarcity in Africa, the whole continent shares only 9% of the fresh water in the world for about 15% of the global population (Mohamed, 2017). According to a study made in 1996 by the United Nations Environment Program (UNEP) the northern part of Africa will face a crisis in water scarcity by the year of 2025.

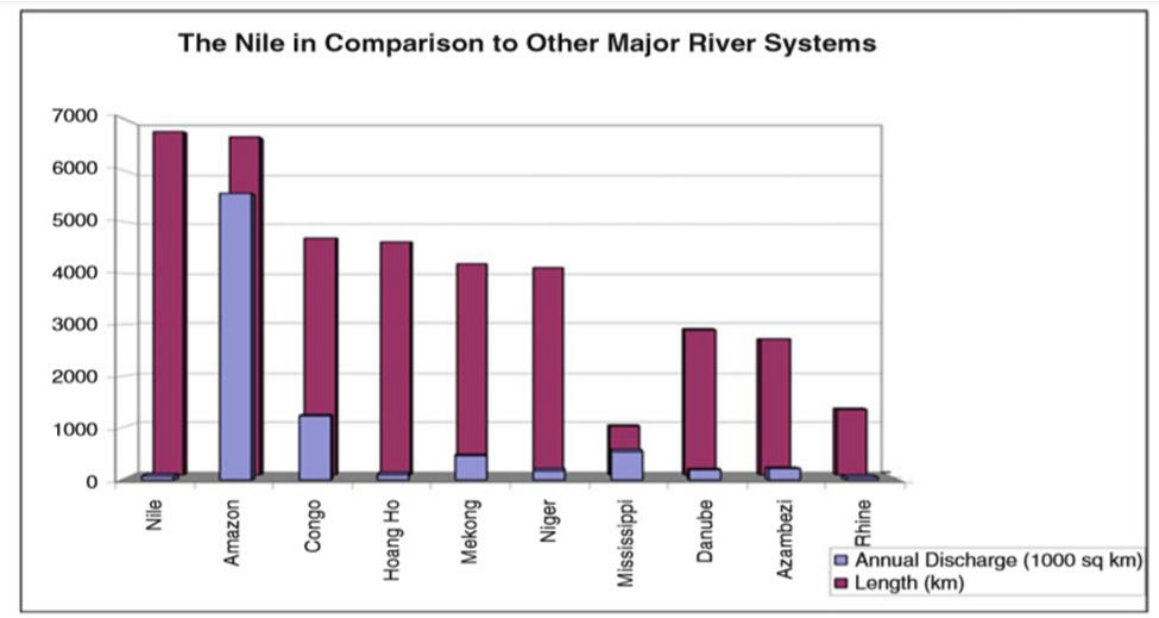

Figure 2.2 The Nile in comparison to another Major Rives(https://www.internationalrivers.org)

Although the White Nile Basin size is five times greater than the Blue Nile Basin, the latter contributes substantially more streamflow to the main Nile River. The total streamflow emanating from the Ethiopian highlands through the Blue Nile and Atbara Rivers accounts for approximately 84% of the inflow to Lake Nasser at Aswan, Egypt. The Blue Nile itself contributes approximately 65% of the total Nile flow into Lake Nasser (Yates & Strzepek, Modeling the Nile basin under climate change, 1998). The grand Ethiopian Renaissance dam (GERD) is an ambitious hydropower project that is being constructed on the Blue Nile, close to the border between Ethiopia and Sudan. It will have a reservoir capacity of 74 billion cubic meters (BCM); and when fully operational, it will have a power capacity of 6,000 MW. Construction began in 2011 and it is expected to start function during 2020 (Ethiopian Electric Power Corporation 2013). Ethiopia is endowed with significant water resources, providing an estimated hydropower potential of 45,000 MW nationally (Salman, 2013). Seeking sustainable economic growth, Ethiopia aims to exploit this potential and is undertaking a larger domestic product (GDP) growth rate (Bank, 2006). Since, Ethiopians depend on rainfed agriculture, this variability is closely associated with vulnerability. Therefore, the development of storage may partially buffer the rainfall decreasing due to climate change.

2.2 Aswan High Dam Reservoir

In Egypt, one of the most essential components of the water resource systems is the Aswan High Dam Reservoir (AHDR), also called Aswan High Dam Lake (AHDL). Its function is to regulate the flow downstream of the AHD in relation to the different requirements of the country in terms of water needs (Ahmed & Ahmed , 2008). Moreover, this lake is considered the main source of freshwater for about 85% of its population (Elsahabi MA & Negm , 2016) . The Aswan High Dam Lake (AHDL) is one of the greatest man-made reservoirs in the world, created after the construction of the AHD. This reservoir has an extension of 500 km along the Nile River from the southern part of Egypt to the northern part of Sudan. The area it covers is around 6,000 km2, of which two-thirds (known as Lake Nasser, 350 km) is located in Egypt and one-third (called Lake Nubia, 150 km), in Sudan (Ahmed & Ahmed , 2008) as shown in Figure 2.3.

Figure 2.3 Location map of Aswan High Dam, Lake Nasser, and Lake Nubia

The AHDL designed storage capacity (162 billion m3) is distributed as follows [3]:

• 31.6 billion m3: dead storage between levels of 85 m and 147 m

• 90.7 billion m3: live storage capacity between levels of 147 m and 175 m

• 39.7 billion m3: flood control storage capacity between levels of 175 m and 182 m

2.3 GERD Project

The US Bureau of Reclamation (1964) conducted a study on behalf of the government of Ethiopia that identified four potential sites on the Blue Nile for dam projects, one of them is called the Grand Ethiopian Renaissance Dam (GERD), which is located approximately 500 km North West of the capital Addis Ababa, in the region of Benishangul – Gumaz. The GERD will be the largest dam in Africa: 1,800 m long, 155 m high and with reservoir storage of 74,000 billion m3.

2.4 GERD and the Threat of Egyptian Water Resources

At the Egyptian domestic level, experts and specialists stressed that the dam has significant risks on all aspects: water, agriculture, environment, economics, society, and availability of electricity. A report issued by the Technical Committee for the Dam Assessment on May 2013 shows details of the dam and its negative effects on Egypt (Sharaki , 2013). Additionally, studies conducted by professors of Cairo University, which have been validated by international studies, verify that the expected negative effects of GERD on Egypt's water security are elevated and may be catastrophic especially during the filling period of the dam. If the filling is synchronized with a flood period below the average, the effects will be devastating. Egypt is expected to be unable to get its share of water during the filling period with an average deficit of 20% of the quota (11 BCM) and a maximum deficit of 34% (19 BCM), which extends to 6 years (Group of Nile Basin, 2013). These impacts are exacerbated as climate changes increase (Liersch & Koch). The filling of the lake behind this dam with this huge volume of water – even if it is estimated that it could happen within 5 years – means deducting 15 BCM each year from the share of Egypt and Sudan. More accurately, it will be from Egypt's share only since Sudan's dams (Khashm el-Girba, Rusairis, Sennar, and Marwa) reserve Sudan's share of water before it reaches Egypt. If Ethiopia decided to fill the lake in just 3 years, it implies deducting 25 BCM per year, which means major destruction to Egypt (Zhang , Erkyihum , & Block , 2016). GERD preliminary technical studies indicate that the greatest risk related to the dam is that it is located on a very rugged slope. Therefore, the probability of its collapse is very high (El-Nashar & Elyamany, 2017). Moreover, its safety coefficient is not more than 1.5 degrees compared to the High Dam 8 degrees' safety factor. The report emitted on May 2013 from the International Technical Committee concerned with assessing the impacts of the Renaissance Dam confirmed the lack of scientific studies needed for the GERD project, mainly the apparent imbalance in engineering studies on GERD safety (El-Nashar & Elyamany, 2017).

2.5 GERD and the Threat of the Egyptian Agricultural Sector

Egypt is located at the south eastern corner of the Mediterranean and covers an area of one million square kilometers. Egypt measures 1262 km from west to east (Mediterranean coast), and 1073 km between latitudes 22° and 32° N. This latitudinal location means that most of the country falls within Africa's dry desert region, except for a narrow strip along the northern coast which experiences a Mediterranean type of climate. Egypt is practically rainless; its agriculture depends mainly on irrigation. The mean annual rainfall of 18 mm ranges from 0 in the desert to 150 mm per year along the Mediterranean coastal region. During summer, temperatures are extremely high, reaching 38°C to 43°C with extremes of 47°C in the southern and western deserts (mean daily maxima). The Mediterranean coast has cooler conditions with 32°C as mean daily maximum (FAO, 2005).

Egyptian population has almost doubled during the last thirty years, recording a 38 million increment in inhabitants, from 42 million in 1990 to almost 80 million in 2010. Inhibited areas in Egypt are about 6% of its total coverage, mainly concentrated in the Nile Delta and around the Nile Valley along with scattered development zones along the Mediterranean and Red sea coasts, the Sinai Peninsula, and few oases in the Western Desert**Invalid source specified.**. The former reflects the sever aridity prevailing across most of the country. Increasing population, increasing population density, limited water resources, and hyper-aridity represent major development constraints in Egypt. Climate-induced changes especially more frequent occurrence of extreme events adds another potential constraint**Invalid source specified.**.

2.5.1 Freshwater supply

One of the most difficult challenges in Egypt is the fully dependency on the water from the Nile river: the Egyptian share from the Nile is about 55.5 billion cubic meters (BCM) with a population of more than 100 Million people. According to that percentage, there is already a problem of water shortage in Egypt because the person share of water is less than 1000 m^3/year **Invalid source specified.**. According to the dry climate of Egypt there is no rainfall water considered to be used, average rainfall in Egypt is estimated at 1.8 BCM per year (Ibrahim, 2017). Currently, the overall average annual rainfall in Egypt is about 18 mm mainly occurring at the northern coast which receives about 150 mm of precipitation per year. In the southern Upper Egypt, Sinai, and along the Red sea coast events of measurable rainfall may be encountered once every 5 to 9 years, sometimes developing into very short, but destructive, flash floods. Precipitation which occurs in

winter and late autumn accounts for 1.3 BCM/y of internal renewable water resources recharging shallow aquifers. The Nile River supplies about 97% of the annual renewable water resources in Egypt. Out of the Nile ‘s average natural flow of 84.0 km^3/y reaching Aswan, a share of 55.5 BCM/y is allocated to Egypt according to the Nile Water Agreement (1959). The Agreement also allocates a share of 18.5 BCM/y to Sudan; while about 10 BCM/y is lost in evaporation from the high dam reservoir (Lake Nasser) Figure 2.4 (Wagdy, An overview of Groundwater Management in Egypt, 2010), (FAO, 2007). Thus, the total renewable water resources of Egypt are estimated at 56.8 BCM/y. The latter amount of supply is constant and incremental possibilities are not foreseen for the short term.

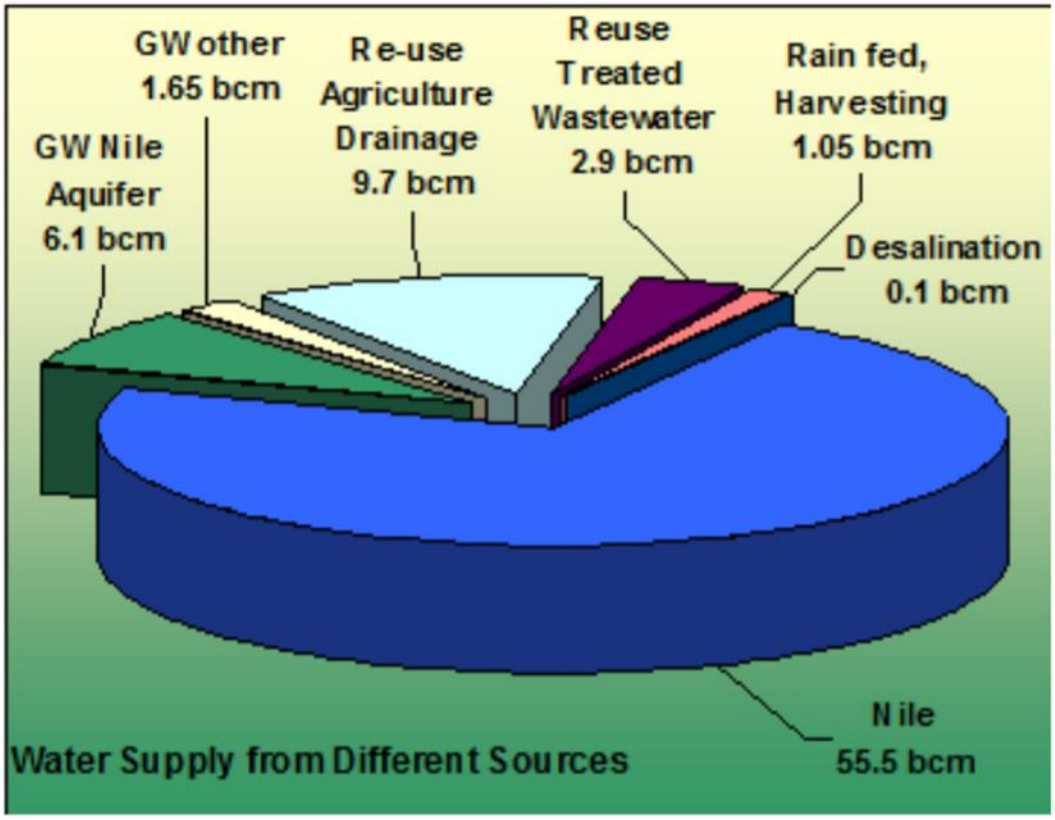

Figure 2.4 Sources for water supply

Groundwater utilization has been steadily increasing in Egypt for the last twenty years. A designated sector for groundwater management has been established at the Ministry of Water Resources and Irrigation to coordinate, develop, and rationalize the national groundwater utilization. There are four major groundwater systems in Egypt Figure 2.5, namely, the Nile Aquifer, Egypt has four different groundwater aquifers: the Nile Aquifer, the Nubian Sandstone

Aquifer, the Moghra Aquifer and the Coastal Aquifer (Ibrahim, 2017). The underground water represents less than 5% of the water usage in Egypt, because it is nonrenewable water resource that people cannot depend on. The first aquifer contains groundwater in the Nile Valley and Delta region. The second aquifer category is in the "Western Desert-Nubian Sandstone Aquifer". Non-renewable groundwater utilization is estimated at a rate of 1.65 Billion m3 /year (BCM/year). It is mostly located at the Western Desert Oases with 0.5 BCM/yr. On the other side, the groundwater abstractions in Delta, Sinai and New Valley regions is about 5.1 BCM/yr. It is estimated that about 200,000 BCM of fresh water are stored in the New Valley's Oasis aquifer only. The water is at the depth of 60-100 m around the area of East-Oweinat. In Sinai, groundwater is mainly encountered in three different water bearing aquifers (Abdel-Shafy et al, 2016), the Nubian Sandstone Aquifer, the Moghra Aquifer and the Coastal Aquifer. The Nile aquifer is renewable and underlies the Nile Delta and is characterized by its high productivity and shallow depth of the groundwater table allowing the abstraction of large quantities of water (100-300 m3/hr.) at low pumping cost. Conjunctive use of surface and groundwater is widely practiced by farmers, especially during periods of peak irrigation demands. About 6.1 BCM/y are annually extracted from the aquifer.

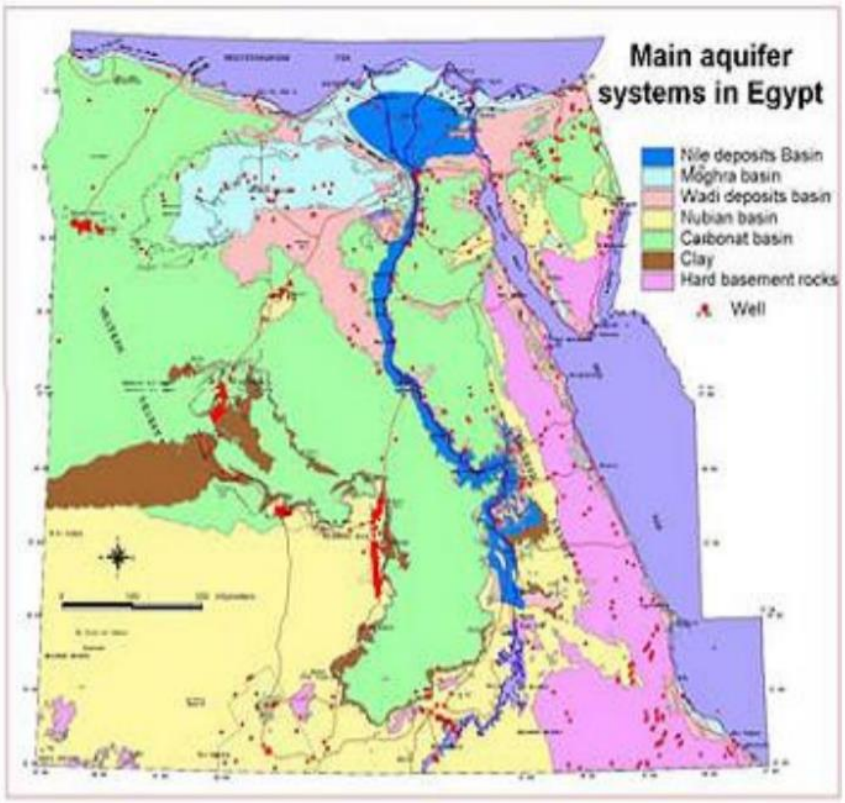

Figure 2.5 Main aquifer systems in Egypt (UNEP/MAP,2011)

2.5.2 Water demand

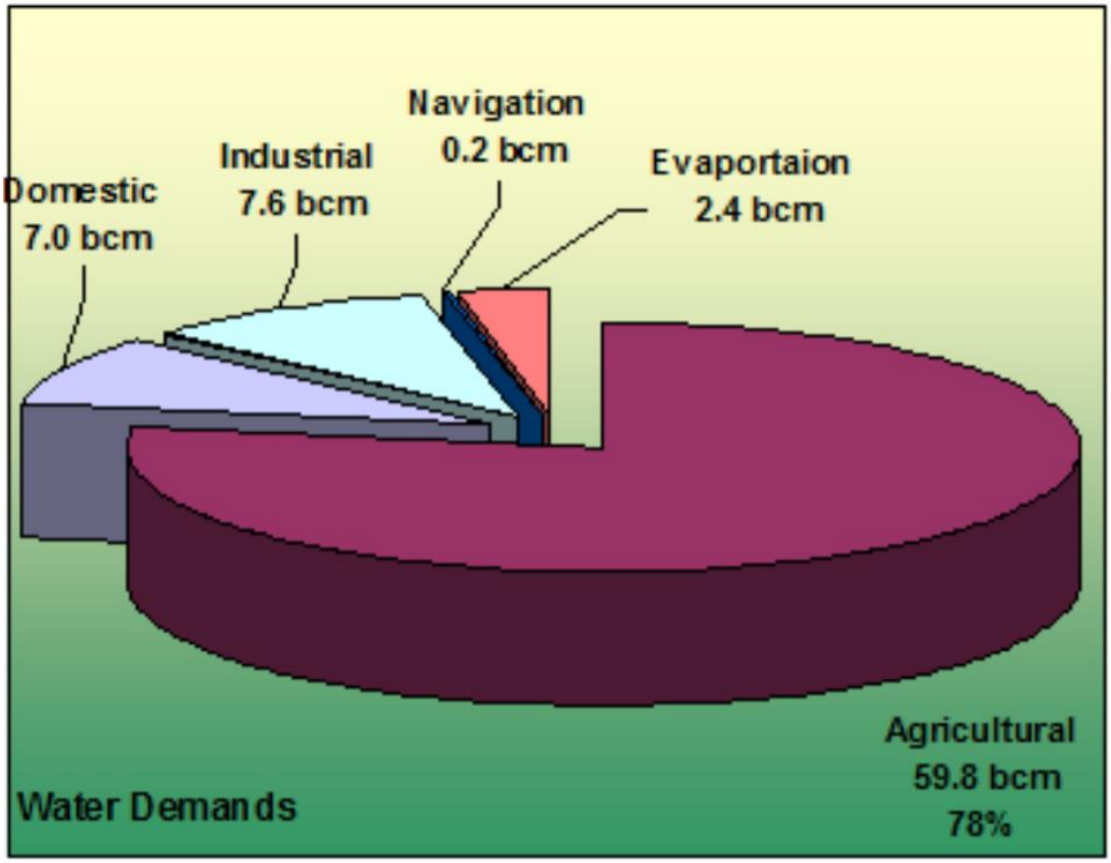

Figure 2.6 Water demand in Egypt (FAO, 2007)

Water in Egypt is used mainly in agriculture, industry, and domestic uses, according to Ibrahim (2017) the forecasted water demand from the year of 1999 till the year of 2025 is illustrated in Figure 2.7. Ibrahim (2017) assumed that the water reduction of the downstream share of Nile River is about 10 BCM constant reduction from the year of 2017 till the year of 2025 which is not very accurate because the water reduction is not a constant rate and the filling of the GERD reservoir was postpone to the year of 2020 as illustrated in section 3 but this study is still useful because it summarizes the water demand as the house hold use, industrial water, River Navigation and as a result the rest of water goes to the agriculture purpose. The navigation and energy (i.e. hydropower) sub-sectors are instream users; meaning that they utilize the Nile/irrigation distribution system, but they are not net consumers of the water resources. Drainage water spilled to the Mediterranean Sea and the desert fringes of the Nile system contributes the water needed to maintain the

ecosystem/habitats of the northern Delta/Lakes. Evaporation losses from the 31,000 Km-long water conveyance networks is estimated at about 2.4 BCM/y, Figure 2.6, (FAO, 2007).

Year		1999	2015	2017	2020	2025
Population (Forecast ed from census)	Capita	64158887	82599416	84957493	88494536	94389513
Water deficit due to construction of Ethiopian dam	Billion m^3/yr)	-	-	10	10	10
Water supply	Billion (m^3/yr)	59.2	59.2	59.2-10=48.2	59.2-10=48.2	59.2-10=48.2
	%	100%	100%	100%	100%	100%
Households-Domestic water	Billion (m^3/yr)	3.1	3.99	4.10	4.28	4.56
	%	5.24%	6.74%	8.51%	8.88%	9.46%
Industrial water	Billion (m^3/yr)	4.6	5.92	6.09	6.34	6.77
	%	7.77%	10.00%	12.63%	13.15%	14.05%
River Navigation and water mouth out flow	Billion (m^3/yr)	1.8	1.8	1.8	1.8	1.8
	%	3.04%	3.04%	3.73%	3.73%	3.73%
Total	Billion (m^3/yr)	9.5	11.71`	11.99	12.42	13.13
	%	16.05%	19.78%	24.88%	25.77%	27.24%
Agriculture-Irrigation water	Billion (m^3/yr)	49.7	47.49	48.2-11.99= 36.21	48.2-12.42= 35.78	48.2-13.13= 35.07
	%	83.95%	80.22%	75.12%	74.23%	72.76%

Figure 2.7 the expected water needs in Egypt till the year of 2025 (Ibrahim, 2017)

Water resources management, hydraulic control, channel design, distribution networks, and water discharge monitoring has been practiced by Egyptians for over 5000 years. The total dam capacity is currently about 169 km3 mainly attributed to the reservoir of the Aswan high dam. About 90% of the Nile ‘s hydro-potential has been exploited to generate about 12 T wh. The irrigation potential is estimated as 4.4 million ha. (UNEP/MAP Regional Activity Centre, 2011).

2.5.3 Water sector governance in Egypt

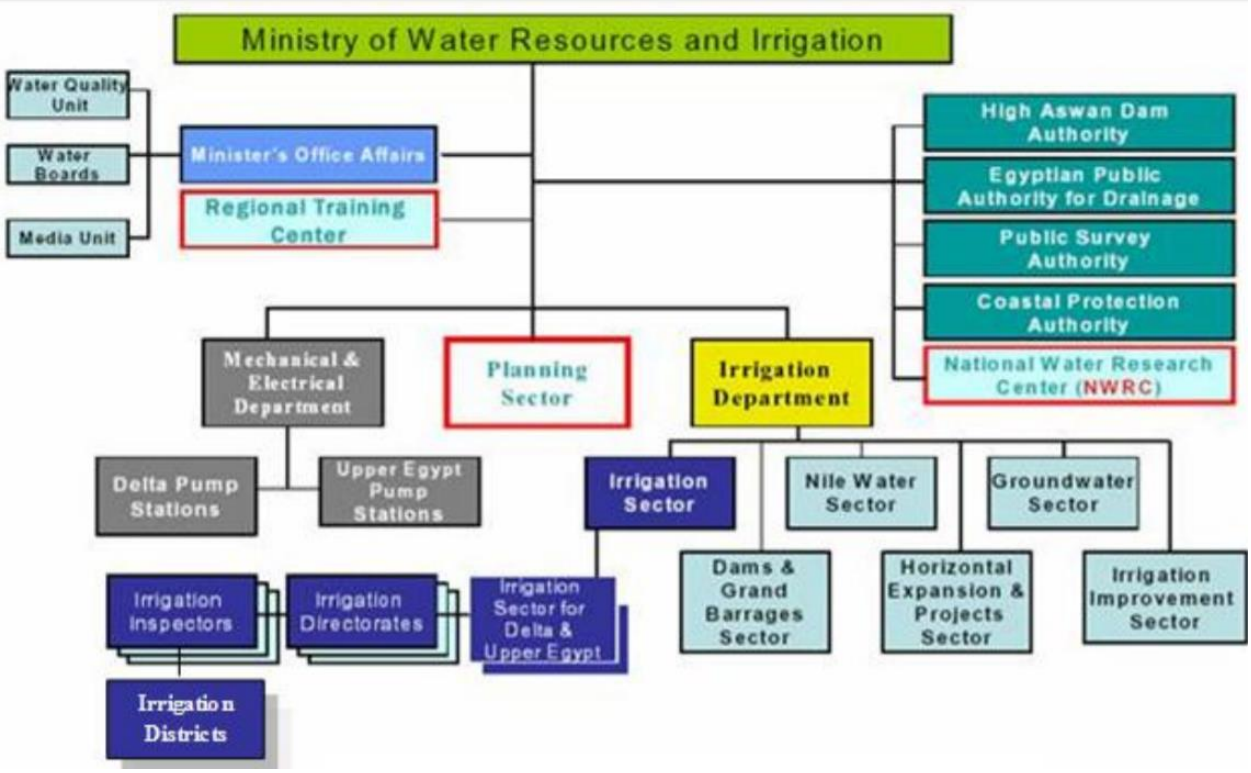

Figure 2.8 Water Sector Governance in Egypt (UNEP/MAP,2011)

Five main socio-economic sectors are dependent on the available scarce water resources for their development; namely agricultural, industrial, municipal, navigation, and power generation sectors. The cultivated and cropped areas have been increasing over the past few years and will continue increasing due to the Government policy to add more agricultural lands. Three major governmental entities influence the management of water resources in Egypt. These are: (i) The Ministry of Water Resources and Irrigation, (ii) The Ministry of Agriculture and Land Reclamation, and (iii) The Ministry of Housing. The Ministry of Water Resources and Irrigation is responsible for collection and disposal of agricultural drainage water, monitoring and assessment of water quality of the various water sources, and protecting the coastal lakes and the shoreline. The Ministry of Agriculture and Land Reclamation (MALR) is involved in improving agricultural activities and land reclamation, including water management at the on-farm level. The Ministry of Housing, Utilities and New Communities (MHUNC), provides water supply and sanitation services to the municipal and industrial subsectors. Some 11 other ministries participate by different degrees in auxiliary management and operation of part of the irrigation and drainage systems such as Ministry of Health and Population (MoHP), the Ministry of State for Environmental Affairs, and the

Ministry of Local Development (MoLD). Figure 2.8 represents the structure of MWRI (UNEP/MAP Regional Activity Centre, 2011).

2.5.4 Existing national water policies and strategies

The water policies of the 1970‘s and early 1980‘s gave a significant advantage to new lands development. However, recent changes in price and other policies particularly the reduction/elimination of government fertilizer and energy subsidies place farmers in the new land at a disadvantage (IDSC , 2007). During the seventies and early eighties of the last century policies have been directed towards water supply management. At present, integrated water resources management, which seeks an efficient blend of all available resources (fresh surface water, ground water, precipitation and drainage water) to meet demands of the full range of water users (including agriculture, municipalities, industry and in-stream flows) is becoming an integral part of MWRI‘s policy vision to meet these challenges. An extensive coordination effort among concerned government institutions and the active participation of water users in planning, management and operation of water collection and distribution systems is required. Integration also necessitates the establishment/enhancement of the legal basis for water allocation, conservation and protection as well as user participation in water management. To cope with these challenges, the MWRI has developed a national policy with four major pillars of: 1) increasing water use efficiency; 2) water quality protection; and 3) pollution control and water supply augmentation and 4) Institutional restructuring (NWRP, 2004).

2.5.5 The agricultural system in Egypt

The Egyptian agricultural year starts in April and comprises three seasons; (i) Winter season: Dec 1st to Apr 1st, (ii) Summer season: Apr 1st to Aug. 1st, and (iii) Flood season (Niley): Aug 1st to Dec 1st. Main summer crops are corn, cotton, rice and sugarcane. Main winter crops are wheat, clover, barley and beans. Corn fodders and vegetables are usually grown during the Niley season. The largest consumers of irrigation water are Rice and Sugarcane because they have high water requirements in addition to occupying a considerable area. The average crop consumptive use for year 99/2000 was estimated to be 41.441 billion cm. The total diverted water to agriculture from all sources (surface, groundwater, drainage reuse, and sewage reuse), which includes conveyance, distribution, and application losses, in 99/2000, was about 60.731 Billion cm.

There is no doubt that the water shortage will affect the whole downstream region but this study concerns about the main affected zones by the water crises. One of these regions is the south part

of Egypt where there is the High dam in Aswan and lake Nasser, the water shortage may result in a reduction on the electricity production from the Aswan High Dam. Also, the so called Toshka Valley where there are the four Toshka artificial lakes which were constructed to reach more than its full capacity of Lake Nasser, when its level rises. But, after the construction of the GERD, the water share of Nile River will be less and there will be no chance for Lake Nasser to reach its full capacity so a project like Toshka Valley will be threatened by water shortage. The other part affected severely by the water shortage crises is the northern part of the Nile River where there is the Delta region, it is one of the oldest Deltas in the world which is already threatened by the salinization of the sea water from the Mediterranean sea and soil degradation**Invalid source specified.**

Food and Agriculture Organization of the United Nations

Global Map of Irrigation Areas
EGYPT

Governorate	Area equipped for irrigation, area actually irrigated		
	total (ha)	with groundwater (ha)	with surface water (ha)
Al Bar al Ahmar	0	0	0
Al Buhayrah (Behera)	623 825	14 715	609 110
Al Daqahliyah (Dakahlia)	268 254	6 328	261 926
Al Fayyum (Fayoum)	181 357	4 278	177 079
Al Gharbiyah (Gharbia)	165 262	3 898	161 364
Al Iskandariyah (Alexandria)	64 740	1 527	63 213
Al Jizah (Giza), East	74 654	1 761	72 893
Al Jizah (Giza), West	10 753	10 753	0
Al Minufiyah (Menoufia)	134 662	3 176	131 486
Al Minya (Menia)	202 978	4 788	198 190
Al Qahirah (Cairo)	8 062	190	7 872
Al Qalyubiyah (Kalyoubia)	79 989	1 887	78 102
Al Wadi/Al Jadid	49 999	49 999	0
As Ismailiyah (Ismailia)	87 945	2 074	85 871
As Suways (Suez)	7 998	189	7 809
Ash Sharqiyah (Sharkia)	333 729	7 872	325 857
Aswan	61 674	1 455	60 219
Asyiut	141 719	3 343	138 376
Beni Suwayf (Beni-Suef)	117 858	2 780	115 078
Bur Said (Port Said)	10 345	244	10 101
Dumyat (Damietta)	46 067	1 087	44 980
Janub Sina (South Sinai)	3 394	3 394	0
Kafr-El-Sheikh	265 731	6 268	259 463
Matruh	135 296	135 296	0
Qina	158 055	3 728	154 327
Shamal Sina (North Sinai)	57 831	57 831	0
Suhaj	130 001	3 066	126 935
Egypt total	**3 422 178**	**331 927**	**3 090 251**

Figure 2.9 Map of irrigation Egypt

Currently cultivated land is about 8.5 million feddans (one feddan measures 4200 m2 and is roughly equivalent to one acre) where about 75% belong to the old lands in the Nile Valley, Delta and its peripheries. These lands mainly apply traditional surface irrigation techniques consuming about 87% of the total irrigation demand Figure 2.9. Newly reclaimed lands in several desert areas apply sprinkler and drip irrigation techniques, while conveyance is mainly through lined channels. The total cropped area is equivalent to about 14.2 million feddans with an average national intensification factor of 1.75 (where average land produces more than one crop annually). Figure 2.10 shows the development of arable lands throughout the last century along with corresponding irrigation water demands showing an increase in arable land of about 2.3 million feddans between 1980 and 2010 (UNEP/MAP Regional Activity Centre, 2011).

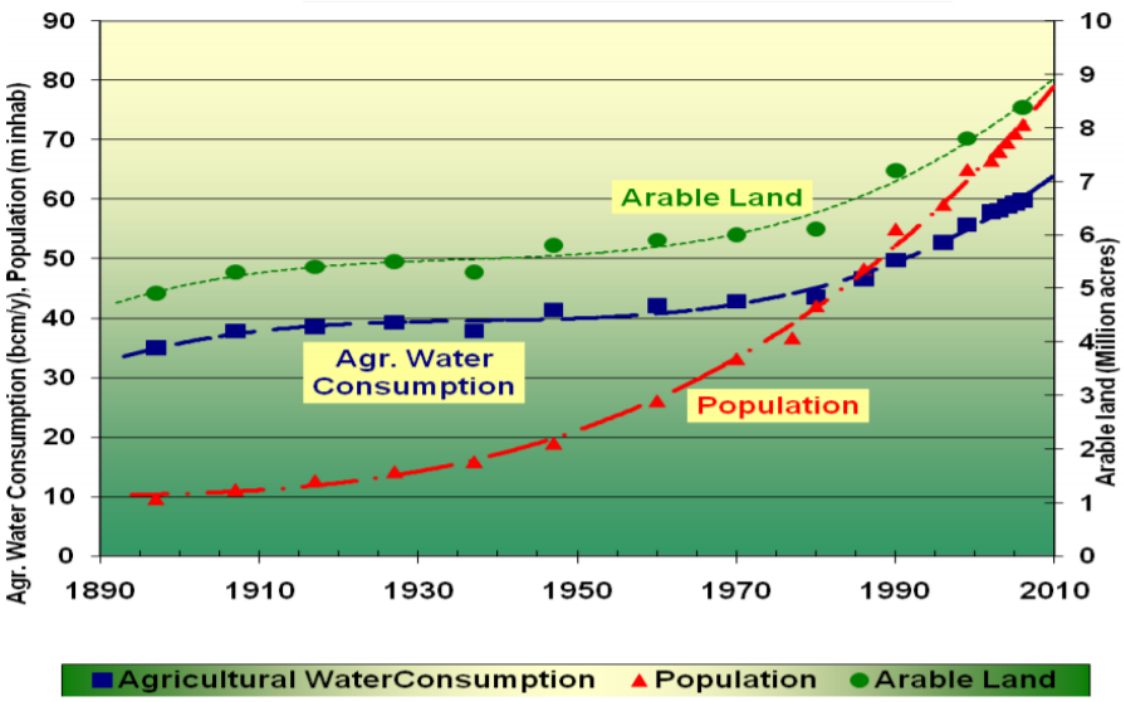

Figure 2.10 Agricultural Water Demands throughout a Century

2.5.6 Challenges and responses to water shortage in Egypt

At present, there are significant challenges to water resources development and use in Egypt. Beginning with a single source of water – The Nile – uncertainties in climate, developments upstream, and population growths have characterized efforts to anticipate potential future water constraints. Municipal and industrial water use is being readily met and agricultural water use yields high levels of production with about 200% cropping intensity. However, the costs for water

services for the next 15 years will be more than triple the current expenditures. Future public sector allocation for such high costs presents a heavy and unsustainable burden for the government budget. Moreover, water quality in a closed system is deteriorating because of pollutants being retained in as part of the recycling and reuse of drainage water, along with poor treatment and regulation of urban and rural sanitation. Stakeholders at the local level are organizing water users associations and water boards to confront the issue and have their voices heard on irrigation and rural sanitation issues.

Experts point out that the shortage of water coming into Egypt due to GERD would have a negative impact on the size of the agricultural area. 3.5 million feddans are expected to be deprived of agriculture. These effects would have serious environmental and social consequences, most notably of which are (El-Nashar & Elyamany, 2017):

1. Each shortage of the Nile water by (4–5) BCM is equivalent to destructing million agricultural acres. In turn, this means the displacement of two million families on the streets in addition to the loss of 12% of agricultural production.

2. Reducing areas of water-consuming crops such as sugarcane and thus increasing the sugar gap by 32%.

3. Salinization of large areas of Egyptian agricultural land due to lack of water allocated to agriculture.

4. Suspending all land reclamation projects and agricultural expansion in Egypt.

5. Increasing the Egyptian food gap to 75% of our total food needs instead of currently 55% (Post-Gazette, 2014).

6. Reduction of Nile water quantities flowing into the Mediterranean Sea and consequently the intrusion of the sea saline water to the Delta lands as well as the underground water.

7. Increasing rates of desertification of agricultural land in addition to increasing pollution concentration in the Nile, canals, and banks due to lack of water flows.

8. Possible disappearance of fish from the Nile for 5 years as well as lack of aquatic biodiversity and also in agricultural soils.

9. Adding additional burden on the Egyptian economy for establishing Mediterranean desalination plants for domestic, industrial, and tourist consumption in the coastal cities of El Arish, Port Said,

Damietta, Rashid, Alexandria, Matrouh, Salloum, Suez, and Safaga, to save the Nile water for agriculture.

10. Affecting negatively on river navigation and tourism.

11. Declining in national income due to the lack of agricultural production accompanied by the decline in rural development rates and the cessation of antipoverty programs (Nigatu & Dinar , 2015).

2.6 Filling Scenarios of GERD and Previous Studies

Various analyses have been conducted regarding the development of the Nile, often focusing on the potential development of the Blue Nile and its likely implications. (Guariso & Whittington, 1987) demonstrated that there is little conflict between the objectives of Ethiopian hydropower and Egyptian and Sudanese agriculture, using a classical multi-objective optimization framework. (Jeuland, Economic implications of climate change for infrastructure planning in transboundary water systems: An example from the Blue Nile, 2010) provided a hydro-economic framework for integrating climate change impacts into infrastructure planning and found a high sensitivity of economic benefits to runoff conditions; this work was furthered with a real-options approach for analyzing the selection, sizing, sequencing and operation of reservoirs within Ethiopia (Jeuland & Whittington, Water resources planning under climate change: Assessing the robustness of real options for the Blue Nile, 2014).

Another class of models developed for the analysis of the Nile Basin is decision support tools, which are generally commissioned by institutions and designed to be used by multiple stakeholders. Models such as the Nile Decision Support Tool (Yao & Georgakakos, 2003) integrate with a database to form a decision support system (DSS) to bring together vast amounts of spatially and temporally discrete and distributed hydrologic data. More recently, the Nile Basin Initiative (NBI), which is commissioned to conduct studies on behalf of member countries, developed the Nile Basin DSS to provide a user-accessible platform that can incorporate a variety of models designed for various purposes (NBI, 2014).

The filling period of the Grand Ethiopian renaissance dam reservoir is a crucial factor of the severity of the impact of water shortage in the downstream country, it could be understood simply that the dam reservoir capacity is 74 billion cubic meters so if the GERD reservoir filling period was 3 years, the water shortage from the downstream countries could be about 24 billion cubic

meters and this is more than 40% if the Egypt's share of the water from the Nile which could lead to a water shortage crises in Egypt. To have a clearer vision of the effect of filling period of the GERD reservoir, in this thesis more than one research was taken into consideration to understand more the extent of the effect of the filling period of the dam reservoir. (Bates, Tuncok, & Barbour, 2013) analyzed specific fixed monthly release patterns ranging from 20.8 to 40.0 BCM/y under three deterministic scenarios (average, moderate drought and severe drought) and using three starting elevations of the HAD. A combination of tools was used in this study, including MIKE BASIN and the RAPSO model (EDF & Scott Wilson, 2007), and separate runs were required to capture the transition of policies from filling to normal operations. Similarly, used MIKE HYDRO to simulate a single historical period of 1973–1978 that represents 'average' conditions to analyze a predefined single six-year filling strategy. This study considered a single hydrologic inflow node on each of the Blue and White Nile tributaries, and included the GERD and HAD, but contained no information on Sudanese reservoirs or any intervening flows. According to (Mohamed, 2017) there are three scenarios for the GERD reservoir filling period. The first one is the three-year filling period: he considered that the initial water level in the Nasser lake is 175, 173or 168 m. Figure 10 shows his results as the effect of the three-year filling period of the GERD on the water level in Nasser lake. Figure 2.11 and Figure 2.12 shows the effect of the five-year and the three-years filling period of the GERD on the water level in Nasser lake.

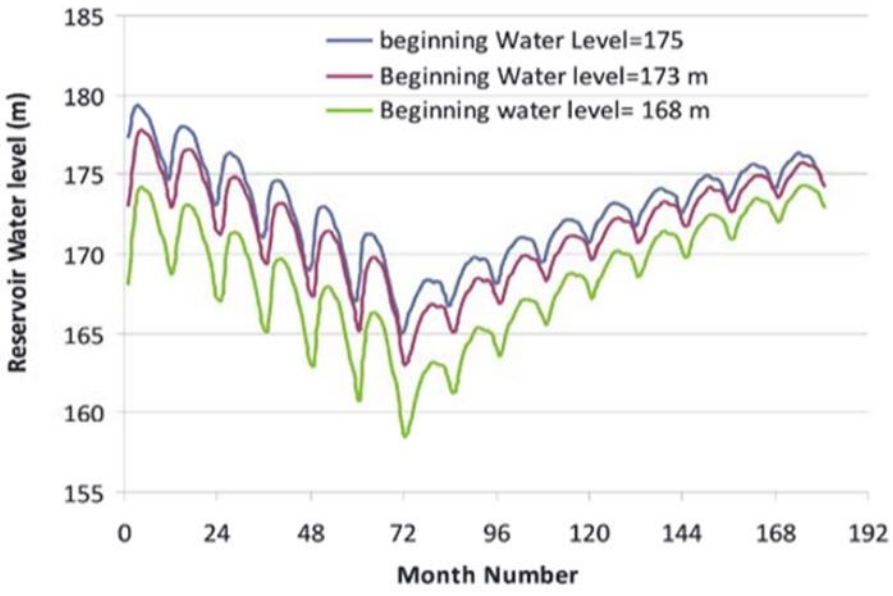

Figure 2.11 The water level in Nasser lake according to 5 years filling scenario (Mohamed, 2017)

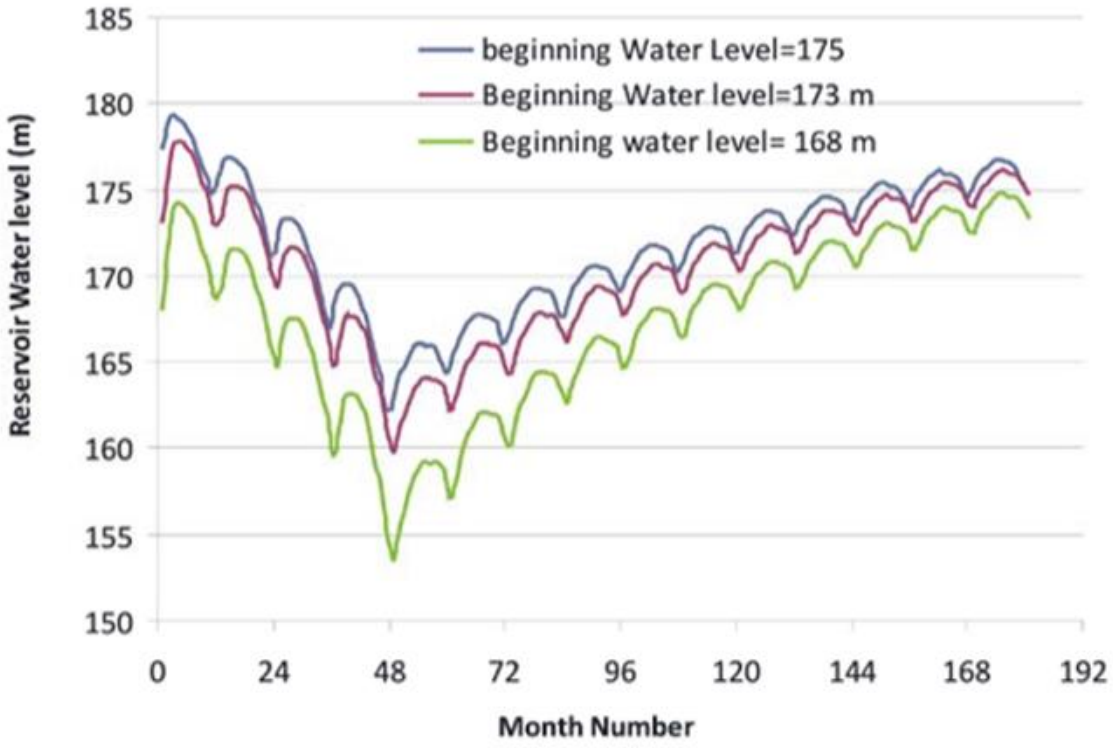

Figure 2.12 The water level in Nasser lake according to 3 years filling scenario (Mohamed, 2017)

2.7 Overview of measuring GERD impact over Egypt

Various analyses have been conducted regarding the development of GERD, often focusing on the hydro power generation of GERD and the impact of GERD on downstream countries, specially Egypt. Many hydrologic models have been developed to simulate the Nile River Basin, the expected filling scenarios of GERD and the potential reduction that is going to affect Egypt. Consequently, most studies expected a big impact on Egypt agriculture due to the construction of GERD. While most studies focused on the hydrologic models, this thesis focused on measuring the impact of GERD on Egypt's agriculture by analyzing the satellite images of Delta Region and comparing the EVI (Enhanced Vegetation Index) in different years using remote sensing. The enhanced vegetation index (EVI) was considered to evaluate the vegetation signal with improved sensitivity in high biomass regions and improved vegetation monitoring through Remote Sensing (Huete , et al., 2002). In this thesis, agricultural characteristics of Delta region have been defined and Delta region has been divided into 5 regions depending on agricultural characteristics. Then, Remote sensing imagery has been processed over the Delta region. Furthermore, a Web

Geographic Information System (WebGIS) Application has been developed in order to share the analysis results between users, organizations and stakeholders. WebGIS (also known as web-based GIS and Internet GIS) denotes a type of Geographic Information System (GIS), whose client is implemented in a Web browser. WebGIS is web-based application that allow sharing GIS through internet (ersi.com, 2020). The Developed Web-GIS Application could help in Effective and fast decision-making mechanism in GERD impact management.

Chapter 3: Vegetation Evaluation for Delta Region through Remote Sensing

3.1 Introduction:

The remote sensing made it easy to get satellite images for anywhere in the world and to make analyses on the satellite images. Then, it allows to measure the changes of the Earth's surface and environment. In this chapter, the analysis by Earth-Engine was performed to detect the changes in the vegetation cover in order to understand the current situation in the downstream area (the Delta Region) of the river Nile. This analysis is mainly based on the calculation of the normalized difference vegetation index (NDVI) and the enhanced vegetation index (EVI). Also, a web-based application has been created with Earth-Engine Application to share the used data, the processing procedures and the results between stakeholders, specialists and different organizations. Using the web-based application stakeholders and different parties can review all the procedures of the analysis, produce modified copies, comment the procedure and the results, correct the analysis and ask for clarifications.

3.2 Earth Engine

Google Earth Engine combines a multi-petabyte catalog of satellite imagery and geospatial datasets with planetary-scale analysis capabilities and makes it available for scientists, researchers, and developers to detect changes, map trends, and quantify differences on the Earth's surface (EarhEngine, www.earthengine.com).

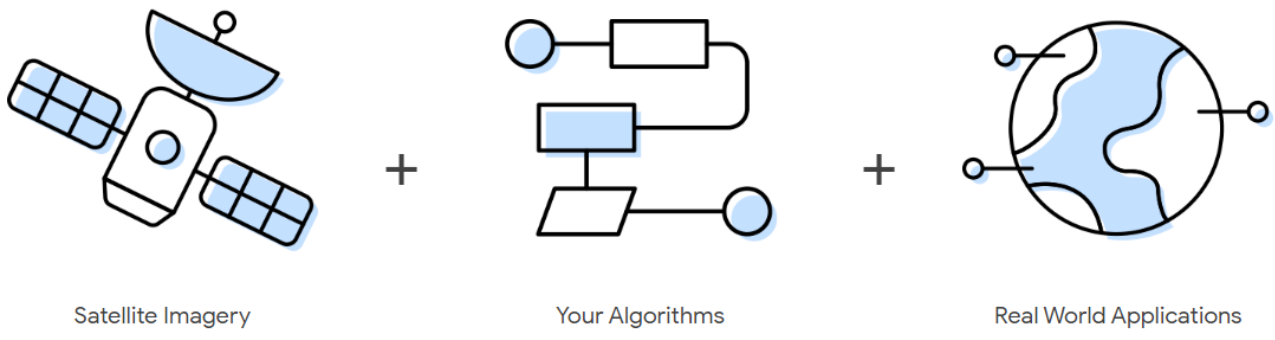

Figure 3.1 Earth-Engine main function

Earth Engine is a platform for scientific analysis and visualization of geospatial datasets, for academic, non-profit, business and government users. Earth Engine hosts satellite imagery and stores it in a public data archive that includes historical earth images going back more than forty years. The images, ingested daily, are then made available for global-scale data mining. Earth Engine also provides APIs and other tools to enable the analysis of large datasets. Earth Engine, on the other hand, is a tool for analyzing geospatial information. It could be used to analyze forest and water coverage, land use change, or assess the health of agricultural fields, among many other possible analyses. The Earth Engine team has worked in close collaboration with Google Cloud to bring the Landsat and Sentinel-2 collections to Google Cloud Storage as part of the Google Cloud public data program. The Google Cloud collections make it much easier and more efficient to access the data directly from Cloud services such as Google Compute Engine or Google Cloud Machine Learning (https://earthengine.google.com/,2020). The data catalog is paired with scalable compute power backed by Google data centers and flexible APIs that let you seamlessly implement your existing geospatial workflows. This enables cutting-edge, global scale analysis and visualization (https://earthengine.google.com, 2020).

3.3 Remote sensing for vegetation monitoring

Remote sensing is the process of detecting and monitoring the physical characteristics of an area by measuring its reflected and emitted radiation at a distance (typically from satellite or aircraft). Remote sensing uses data gathered by satellite sensors that measure wavelengths of light absorbed and reflected by green plants. Certain pigments in plant leaves strongly absorb wavelengths of visible (red) light. The leaves themselves strongly reflect wavelengths of near-infrared light, which is invisible to human eyes. As a plant canopy changes from early spring growth to late-season maturity and senescence, these reflectance properties also change**Invalid source specified.**. Many sensors carried aboard satellites measure red and near-infrared light waves reflected by land surfaces. Using mathematical formulas (algorithms), scientists transform raw satellite data about these light waves into vegetation indices. A vegetation index is an indicator that describes the greenness, the relative density and health of vegetation for each picture element, or pixel, in a satellite image.

3.4 Landsat data

Landsat is an ongoing mission of Earth observation satellites developed under a joint program of the USGS and NASA. The Landsat mission provides the longest continuous space-based record of Earth's land, dating back to 1972 and the Landsat 1 satellite. Starting with Landsat 4, each of the satellites imaged the Earth's surface at a 30-meter resolution about once every two weeks using multispectral and thermal instruments. This collection includes the complete USGS archive from Landsat 4, 5, 7, and 8. It covers their full operational lifetimes, with over four million unique scenes over 35 years:

Landsat 4: 1982 - 1993

Landsat 5: 1984 - 2013

Landsat 7: 1999 - present

Landsat 8: 2013 – present

3.4.1 Landsat 7

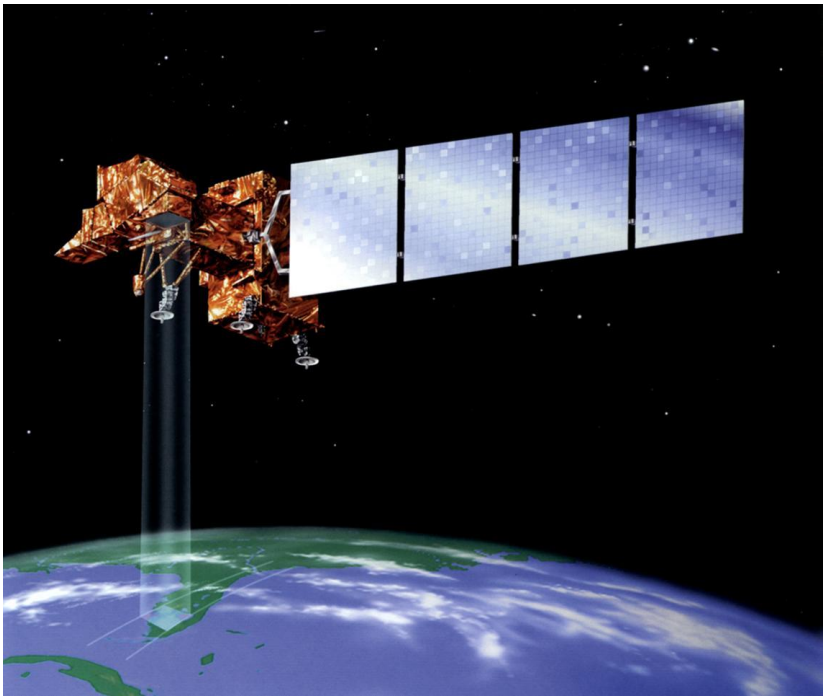

*Figure 3.2 A rendering of Landsat 7**Invalid source specified.**.*

Landsat 7 was launched from Vandenberg Air Force Base in California on April 15, 1999 on a Delta II rocket. The satellite carries the Enhanced Thematic Mapper (ETM+) sensor. The Landsat

7 satellite orbits the Earth in a sun-synchronous, near-polar orbit, at an altitude of 705 km (438 mi), inclined at 98.2 degrees, and circles the Earth every 99 minutes. The satellite has a 16-day repeat cycle with an equatorial crossing time: 10:00 a.m. +/- 15 minutes. Landsat 7 data are acquired on the Worldwide Reference System-2 (WRS-2) path/row system, with swath overlap (or side-lap) varying from 7 percent at the Equator to a maximum of approximately 85 percent at extreme latitudes**Invalid source specified.**.

3.4.2 Landsat 8

Landsat 8 (first known as the Landsat Data Continuity Mission) was launch on February 11, 2013 from Vandenberg Air Force Base, California on an Atlas-V rocket. The satellite carries the Operational Land Imager (OLI) and the Thermal Infrared Sensor (TIRS). The Landsat 8 satellite orbits the Earth in a sun-synchronous, near-polar orbit, at an altitude of 705 km (438 mi), inclined at 98.2 degrees, and circles the Earth every 99 minutes. The satellite has a 16-day repeat cycle with an equatorial crossing time: 10:00 a.m. +/- 15 minutes. Landsat 8 aquires about 740 scenes a day on the Worldwide Reference System-2 (WRS-2) path/row system, with a swath overlap (or side-lap) varying from 7 percent at the Equator to a maximum of approximately 85 percent at extreme latitudes. The scene size is 185 km x 180 km (114 mi x 112 mi)**Invalid source specified.**. The Properties and the technical function of bands are shown in Figure 3.3.

Bands

Name	Resolution	Wavelength	Description
B1	30 meters	0.43 - 0.45 µm	Coastal aerosol
B2	30 meters	0.45 - 0.51 µm	Blue
B3	30 meters	0.53 - 0.59 µm	Green
B4	30 meters	0.64 - 0.67 µm	Red
B5	30 meters	0.85 - 0.88 µm	Near infrared
B6	30 meters	1.57 - 1.65 µm	Shortwave infrared 1
B7	30 meters	2.11 - 2.29 µm	Shortwave infrared 2
B8	15 meters	0.52 - 0.90 µm	Band 8 Panchromatic
B9	15 meters	1.36 - 1.38 µm	Cirrus
B10	30 meters	10.60 - 11.19 µm	Thermal infrared 1, resampled from 100m to 30m
B11	30 meters	11.50 - 12.51 µm	Thermal infrared 2, resampled from 100m to 30m
BQA			Landsat Collection 1 QA Bitmask (See Landsat QA page)

Figure 3.3 Landsat 8 properties and technical function of bands

3.4.3 Convert the Digital Number (DN) to Top of Atmosphere (TOA) reflectance:

The conversion of the Digital Number (DN) to Top of Atmosphere (TOA) reflectance aims at reduction in scene-to-scene variability (Chander et al, 2009). The image data acquired by the satellite sensor do not represent the Earth Surface only, they are affected by atmospheric factor and sun inclination factor. The conversion of the Digital Number (DN) to Top of Atmosphere (TOA)'s target is necessary to clear the image and to represent the earth surface by making some corrections to the satellite raw data. Figure 21 represents the climate factors which affect the satellite image data. There are three benefits of converting the DN to TOA reflectance:

1-the removal of the cosine impact of different solar zenith angles because of the time difference between data acquisitions.

2-TOA reflectance provides for various values of the atmospheric solar irradiance arising from spectral band differences.

3-the TOA reflectance corrects for the variation in the Earth-Sun distance between different data acquisition dates. These variations can be significant geographically and temporally (Chander et al, 2009).

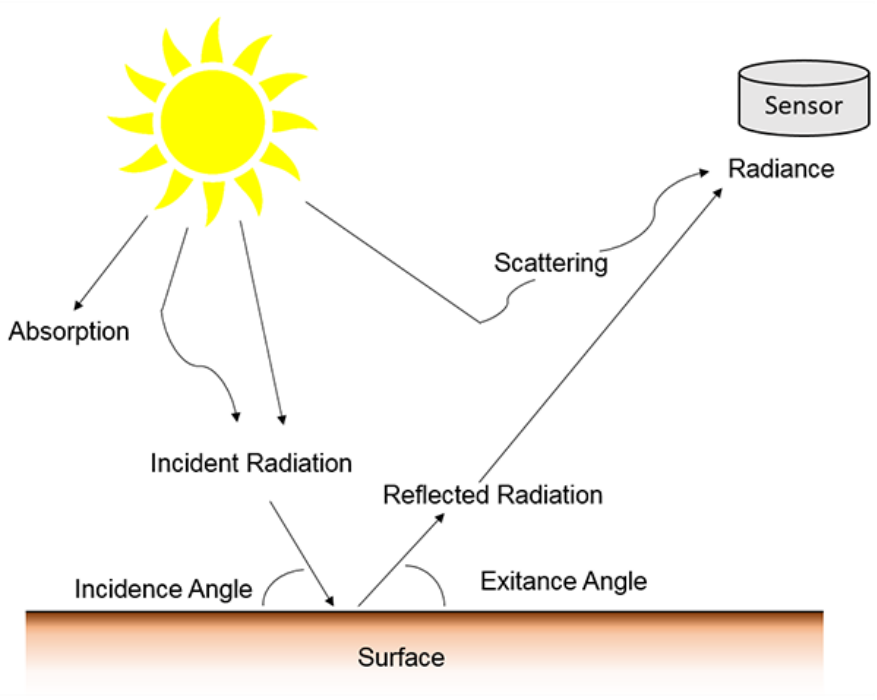

Figure 3.4 The climate factors affect the satellite image data,(gsp.humboldt.edu,2015)

3.4.4 Presence of clouds in the imagery

The presence of clouds is a source of error or lack of precision because clouds and shadows pose a significant barrier for land surface optical and infrared remote sensing image processing and their various applications**Invalid source specified.**. To solve cloud issue, two steps have been done, first masking the cloud, second composing the images, as explained in the following. Landsat 7 and 8 visit the same spot on the Earth once every 16 days. That means over a month period, there will be approximately 2 images and over a year period, there will be approximately 24 images. So, for Monthly evaluation of NDVI or EVI two images have been composited while for annual evaluation 24 images have been composited. Masking the cloud means that masked pixels will be transparent and will be excluded from the analysis. Then, Composing the images means taking the average excluding the masked pixels. For example, over a year period if there are 3 masked pixels as a result of clouds presence , the outcome (the composite) will be the average of the 21 non-masked pixels for this specific point (24-3=21). This technique has the advantage of removing clouds which have relatively unrealistic high values, and shadows (which have relatively unrealistic low value. This technique requires at least two satellite images during a selected period.

3.4.5 The Normalized Difference Vegetation Index (NDVI)

The structure of leaves, evolved for photosynthesis, determines how vegetation interacts with sunlight. Two processes occur within leaves: absorption and scattering of sunlight. Plant pigments (chlorophyll and carotenoids) and liquid water absorb specific wavelengths of light. Scattering is caused by the internal structure of leaves, where the leaf interior is a labyrinth of air spaces and irregularly shaped water-filled cells. Internal scattering of light is caused by differences in the refractive index between air- and water-filled cells and internal reflections from irregularly shaped cells. Green leaves absorb light strongly in the blue and red regions and less so in the green region, hence their green color (Jensen, 2007). No absorption occurs from the upper limit of our vision at 700 nm out to beyond 1300 nm where liquid water begins to absorb strongly Figure 3.5. No absorption means higher levels of reflectance from green vegetation (Tucker & Garratt , 1977).

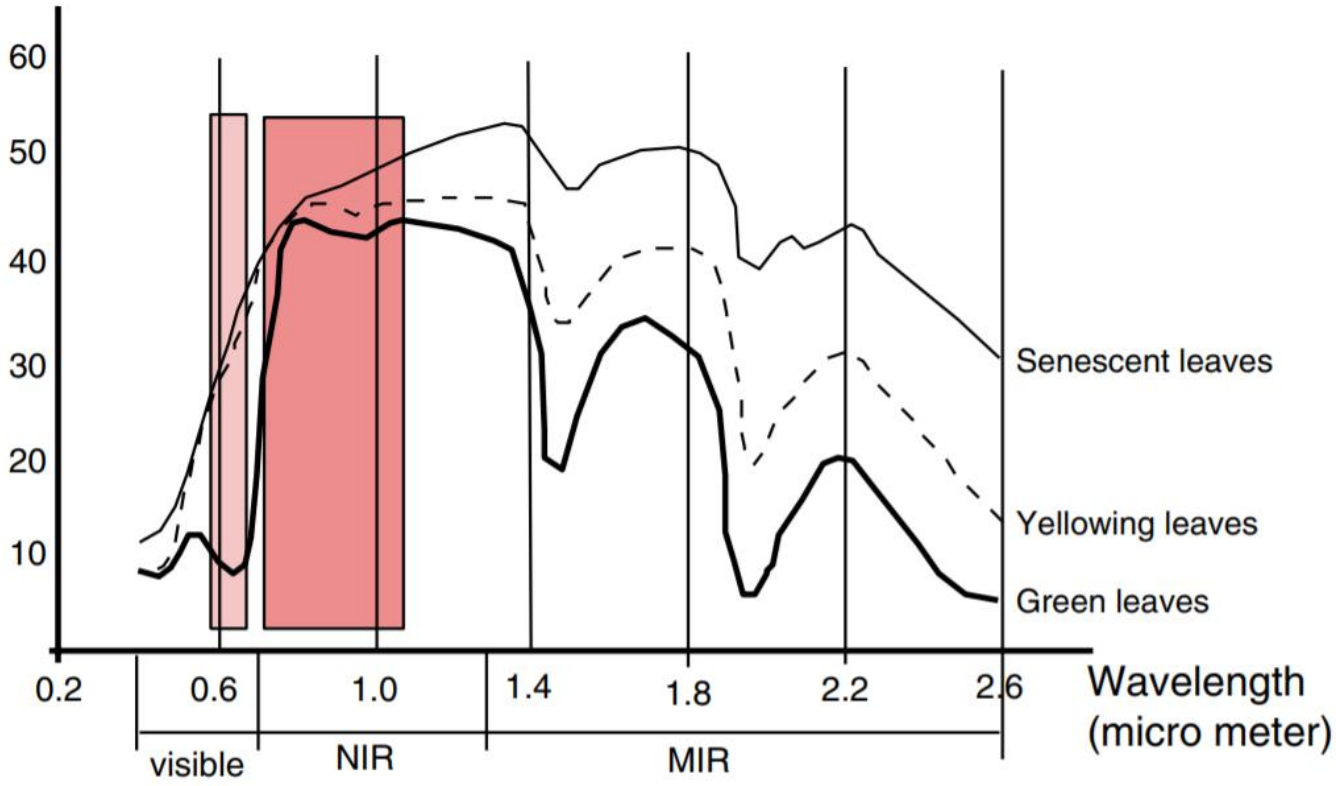

Figure 3.5 Spectral response characteristics of vegetation at three stages of development (Yengoh, Dent, Olsson, & Tengberg, 2015).

The normalized difference vegetation index (NDVI) (Eq. 3.1) is the ratio of the difference between the near-infrared band (NIR) and the red band (R) and the sum of these two bands (Rouse , Haas , & Schell , 1977):

$$NDVI = \frac{Band\ 4 - Band\ 3}{Band\ 4 + band\ 3} \qquad (1)$$

where NIR is reflectance in the NIR and RED is reflectance in the visible red band. The NDVI algorithm takes advantage of the fact that green vegetation reflects less visible light and more NIR, while sparse or less green vegetation reflects a greater portion of the visible and less near-IR. NDVI combines these reflectance characteristics in a ratio so it is an index related to photosynthetic capacity. The range of values obtained is between −1 and +1. Only positive values correspond to vegetated zones, the higher the index, the greater the chlorophyll content of the target (Yengoh, Dent, Olsson, & Tengberg, 2015).

3.5 Enhanced Vegetation Index (EVI)

The enhanced vegetation index (EVI) was developed to optimize the vegetation signal with improved sensitivity in high biomass regions and improved vegetation monitoring through a de-coupling of the canopy background signal and a reduction in atmosphere influences (Huete , et al., 2002). The equation takes the form,

$$EVI = G * ((NIR - R) / (NIR + C1 * R – C2 * B + L)) \quad (2)$$

where ρ are atmospherically corrected or partially atmosphere corrected (Rayleigh and ozone absorption) surface reflectance's, L is the canopy background adjustment that addresses nonlinear, differential NIR and red radiant transfer through a canopy, and C1, C2 are the coefficients of the aerosol resistance term, which uses the blue band to correct for aerosol influences in the red band. The coefficients adopted in the EVI algorithm are, L=1, C1=6, C2=7.5, R=Red, B=Blue, and G (gain factor) =2.5 (Huete , et al., 2002).

3.6 Study Area

Figure 3.6 satellite images that cover Delta regions developed by Earth-Engine

The aim of this thesis is measuring the impact of GERD on Nile River's downstream area. the Delta Region is the last area of river downstream and the biggest agricultural area in Egypt as shown in figure 3.6. Delta Region includes ten governorates: Beheira Governorate, Cairo Governorate, Dakahlia Governorate, Faiyum Governorate, Gharbia Governorate, Giza Governorate, Kafr El-Sheikh Governorate, Menoufia governorate, Qalyubia Governorate and Alexandria Governorate. The ten Governorates have different irrigation systems and agricultural characteristics.

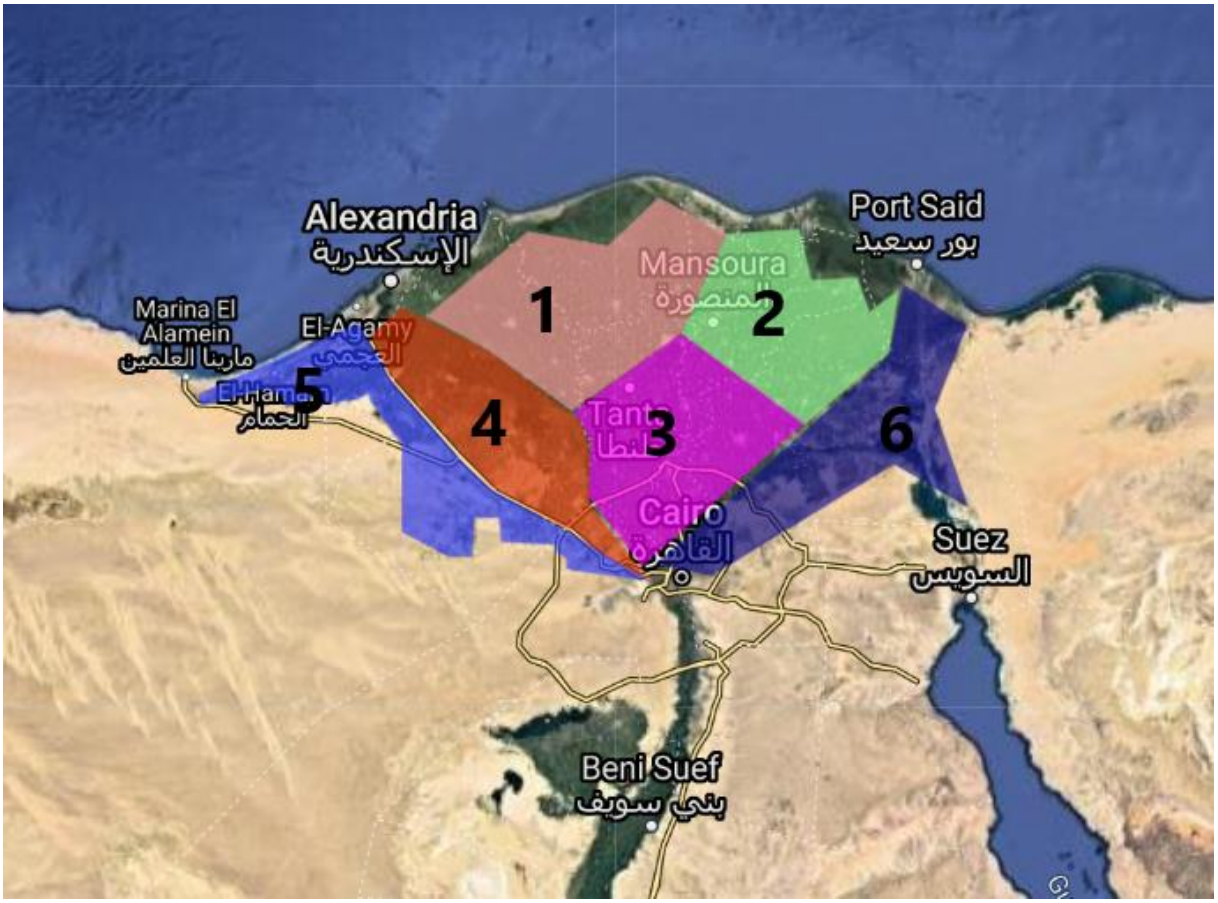

Figure 3.7 Division of Delta regions depending on agricultural system

Agriculture in Egypt depends mainly on two sources of water, Surface water which comes from Nile River and underground water. Underground water has been used in the last decades due to the increasing of food demand and shortage of surface water. Using Data from (FAO) and from agricultural expertise, Delta region has been divided into 6 regions as shown in figure 3.7 depending on the agricultural characteristics, irrigation system and source of water for irrigation (ground water or surface water from Nile river as shown in figure 3.8) regardless governorates division. Considering the storage limitation of underground water and water pumping high cost, underground water dependant areas are using developed irrigation systems such as pivot and drop system to reduce water consumption. Instead, areas depending on surface water use immersion irrigation system.

The regions number 1,2 and 3 use surface water, while region 5 and 6 use underground water. Instead, region 4 uses surface water mainly, however some area in this region use underground water also. The Vegetation Index of each region is calculated in order to evaluate the vegetation

level over the last 20 years. Furthermore, the results are compared with ground data as shown in the following part.

Food and Agriculture Organization of the United Nations

Global Map of Irrigation Areas
EGYPT

Governorate	Area equipped for irrigation, area actually irrigated		
	total (ha)	with groundwater (ha)	with surface water (ha)
Al Bar al Ahmar	0	0	0
Al Buhayrah (Behera)	623 825	14 715	609 110
Al Daqahliyah (Dakahlia)	268 254	6 328	261 926
Al Fayyum (Fayoum)	181 357	4 278	177 079
Al Gharbiyah (Gharbia)	165 262	3 898	161 364
Al Iskandariyah (Alexandria)	64 740	1 527	63 213
Al Jizah (Giza), East	74 654	1 761	72 893
Al Jizah (Giza), West	10 753	10 753	0
Al Minufiyah (Menoufia)	134 662	3 176	131 486
Al Minya (Menia)	202 978	4 788	198 190
Al Qahirah (Cairo)	8 062	190	7 872
Al Qalyubiyah (Kalyoubia)	79 989	1 887	78 102
Al Wadi/Al Jadid	49 999	49 999	0
As Ismailiyah (Ismailia)	87 945	2 074	85 871
As Suways (Suez)	7 998	189	7 809
Ash Sharqiyah (Sharkia)	333 729	7 872	325 857
Aswan	61 674	1 455	60 219
Asyiut	141 719	3 343	138 376
Beni Suwayf (Beni-Suef)	117 858	2 780	115 078
Bur Said (Port Said)	10 345	244	10 101
Dumyat (Damietta)	46 067	1 087	44 980
Janub Sina (South Sinai)	3 394	3 394	0
Kafr-El-Sheikh	265 731	6 268	259 463
Matruh	135 296	135 296	0
Qina	158 055	3 728	154 327
Shamal Sina (North Sinai)	57 831	57 831	0
Suhaj	130 001	3 066	126 935
Egypt total	**3 422 178**	**331 927**	**3 090 251**

Figure 3.8 Egypt's Map of Irrigation (FAO, 2013)

3.7 The Vegetation Index of Region 1

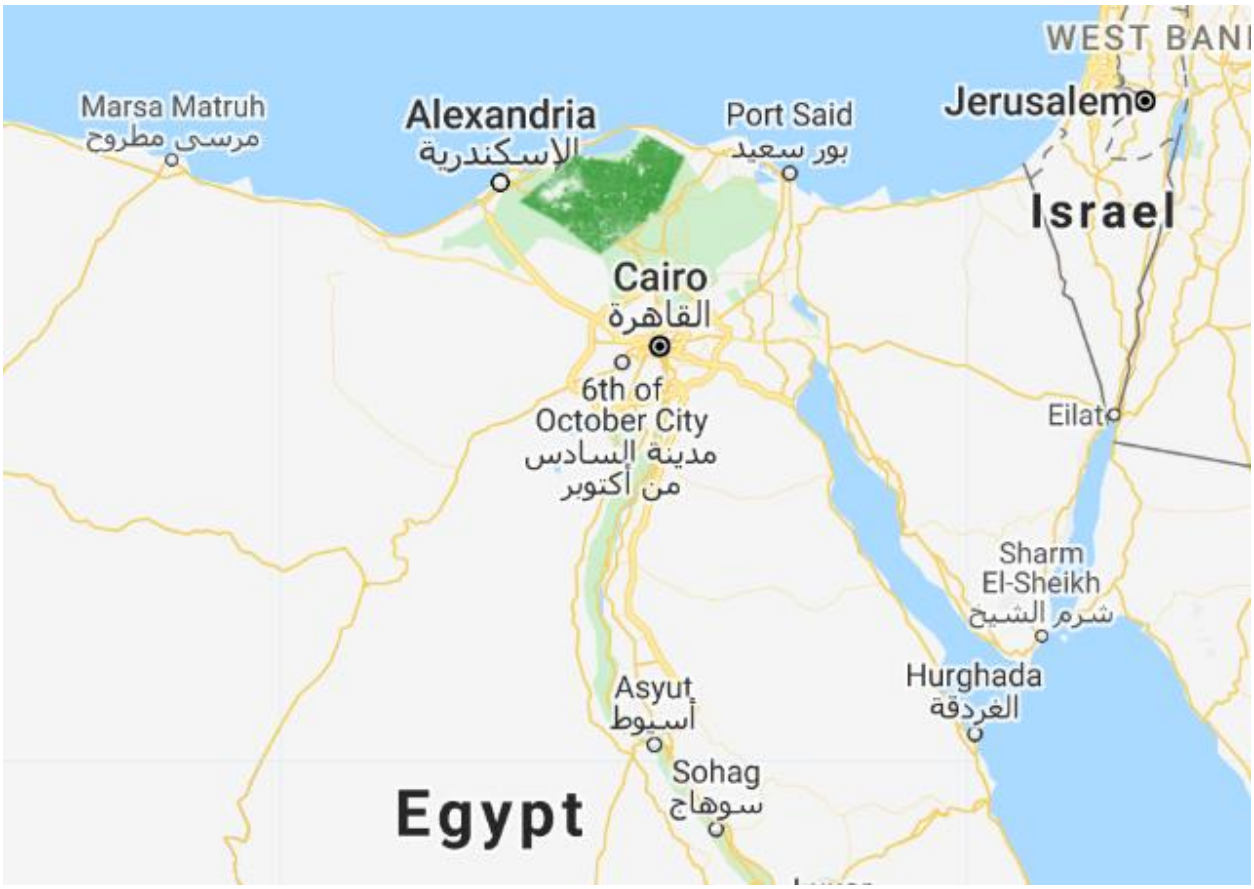

Figure 3.9 region 1

Region 1 is in north of Egypt with an area 6178 km^2. The area is divided into farms that cultivate seasonal crops as shown in Figure 3.10. Region 1 depends on surface water from Nile River for irrigation. Using the computed top-of-atmosphere (TOA) reflectance of Landsat 8 and Landsat 7, composites have been made from orthorectified scenes. The average value of 32 days has been calculated for NDVI and EVI as shown in Figure 3.10, 3.12 and 3.13. The value of each date represents the average value of this date and the following 31 days. These composites are created from all available scenes in each 32-day period beginning from the first day of the year and continuing to the 352nd day of the year. The last composite of the year, beginning on day 353, will overlap the first composite of the following year by 20 days. All images from each 32-day period are included in the composite. Also, the average annual values have been calculated by Landsat 7.

Figure 3.10 High resolution satellite image shows the dense cultivation system in Region 1

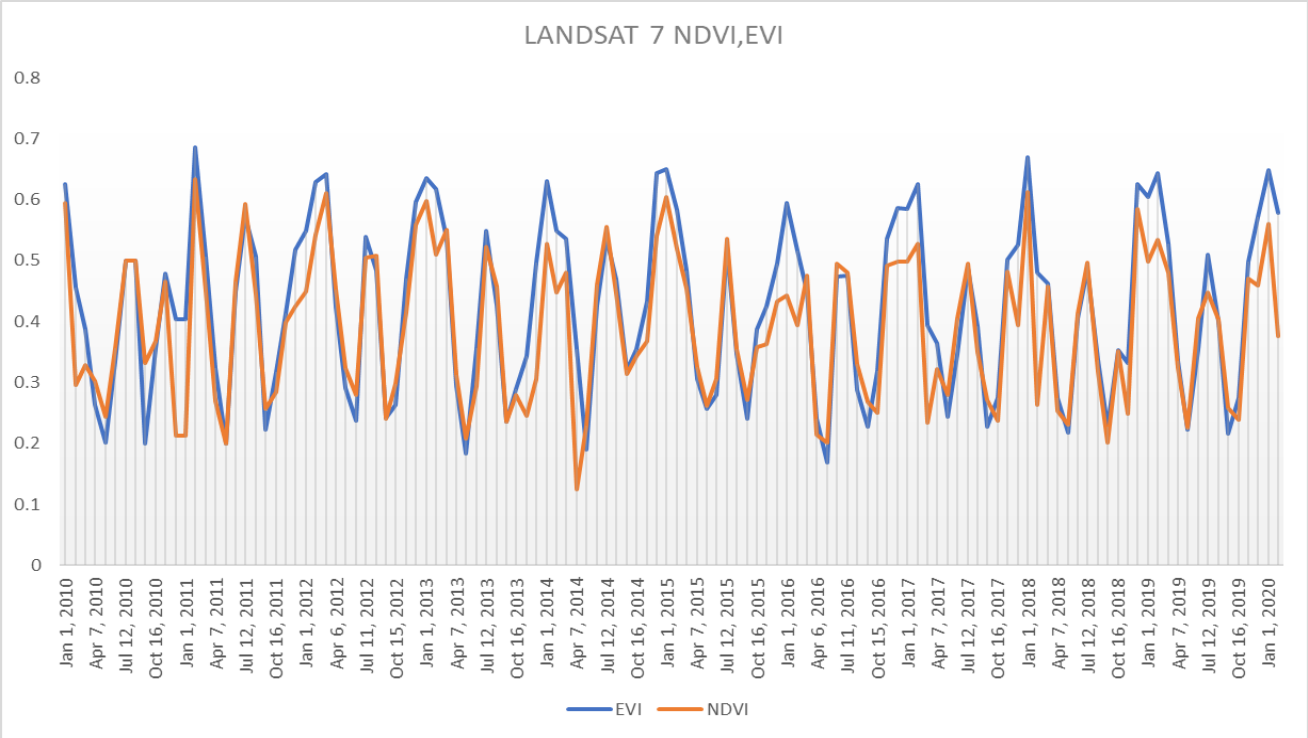

Figure 3.11 Landsat 7, monthly NDVI and EVI for last 10 years

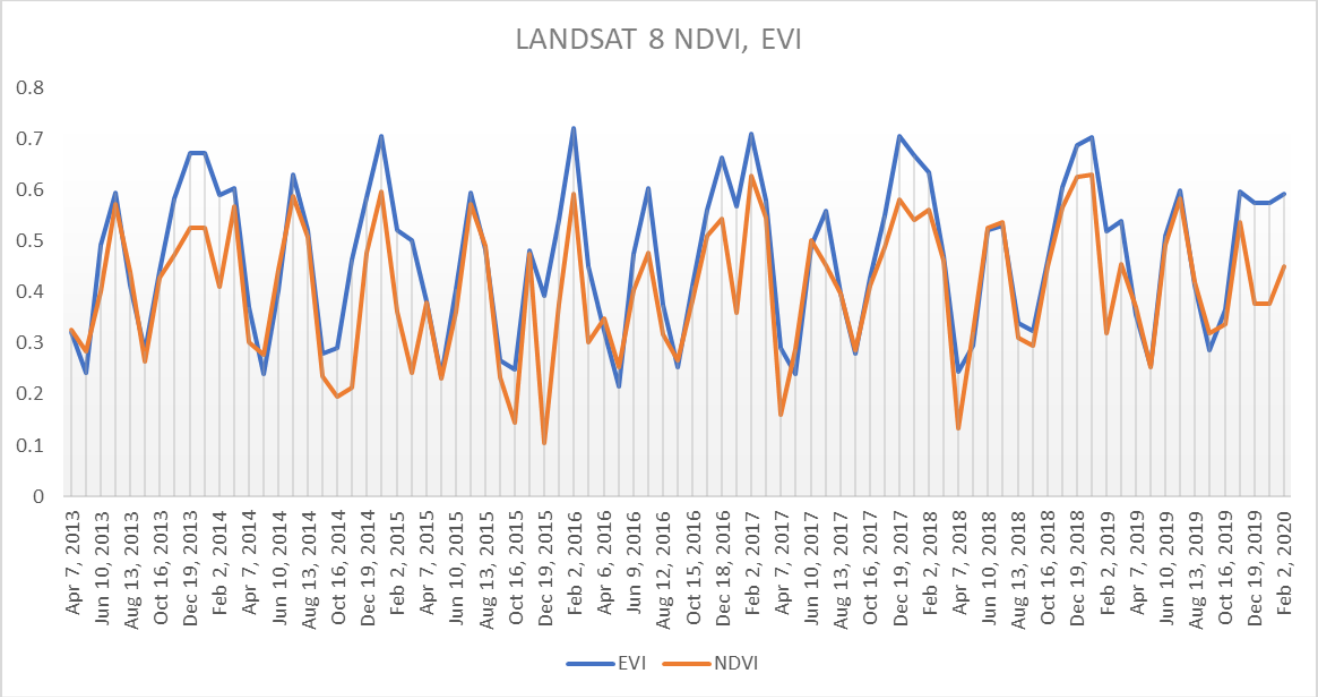

Figure 3.12 Landsat 8, monthly NDVI and EVI for last 7 years

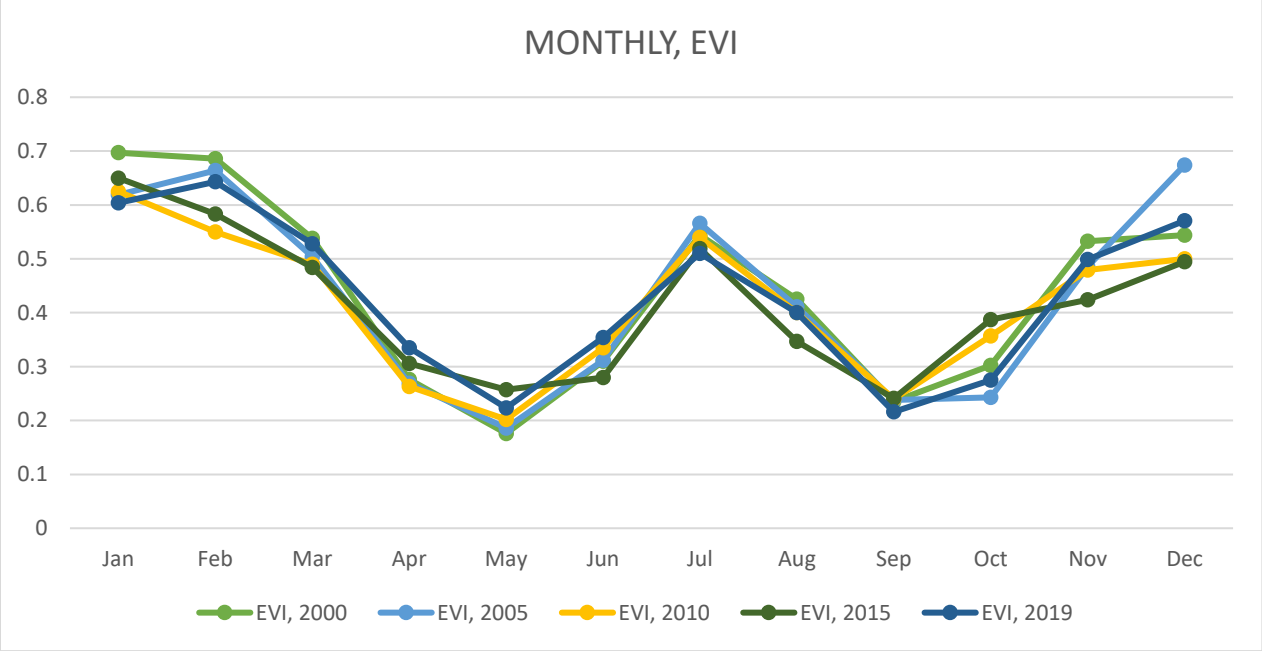

Figure 3.13 Landsat 7, EVI monthly comparison over last 20 years

The results show that September and May have the minimum values over the year because they are the harvest times. While January, February and July have higher values over the year because they are the mid of winter agricultural season and summer agricultural season. The vegetation indices are low in September and then they are incrementally increasing until January which has the highest value over the year. After January, the vegetation indices are incrementally decreasing until May. Then, they start increasing again until July. After that, the vegetation indices are decreasing until September. The Values of January (the mid of winter season) is a bit higher than July (the mid of summer season) beacause the winter season contains big areas of clover, which contains very green leaves and fewer spaces inbetween.

Comparing NDVI and EVI, EVI is more sensitive when measuring the vitality of plants. Moreover, the trend of EVI from Landsat 8 is more coincident with the seasonal agricultural variation trend as explained in previous paragraph and provide more homogeneous results. These results are coincident with (www.vineview.com, 2019) which mentioned “What many do not know, is that NDVI was not designed to measure plant vigour. It was designed to simply detect living vegetation and distinguish it from other matter like rocks, soil, or dead vegetation. With that in mind, it isn’t hard to understand why as an index for measuring vine vigour, NDVI is loaded with potential errors and inaccuracies”. Considering Landsat 7 and Landsat 8, Landsat 8 has higher values comparing to Landsat 7, however both have the same trend and behaviour. Consequently, both of them arrive to the peak at the same time point but with different values. Other studies have got the same results such as (Dandan & Xulin, 2014) which mentioned “When comparing Landsat 7 and 8 NDVI in grasslands, Landsat 8 NDVI is larger than Landsat 7 NDVI when the value of NDVI is low”. Due to the differences between Landsat 7 and Landsat 8, Landsat 7 values cannot be compared with Landsat 8 values in different time or in different location. Landsat 8 has better results but only limited from 2013 until now. Landsat 7 has bigger range of time.

3.8 The Vegetation Index of Region 2

Figure 3.14 Region 2

Region 2 is in north of Egypt with an area 4590 km^2. The area is divided into farms that cultivate seasonal crops as shown in Figure 3.15. Region 2 depends on surface water from Nile River for irrigation. The monthly EVI average has been calculated over the last 20 years to detect the changes of vegetation level over time as shown in Figure 3.16 and 3.17.

Figure 3.15 High resolution satellite image shows the dense cultivation system in Region 2

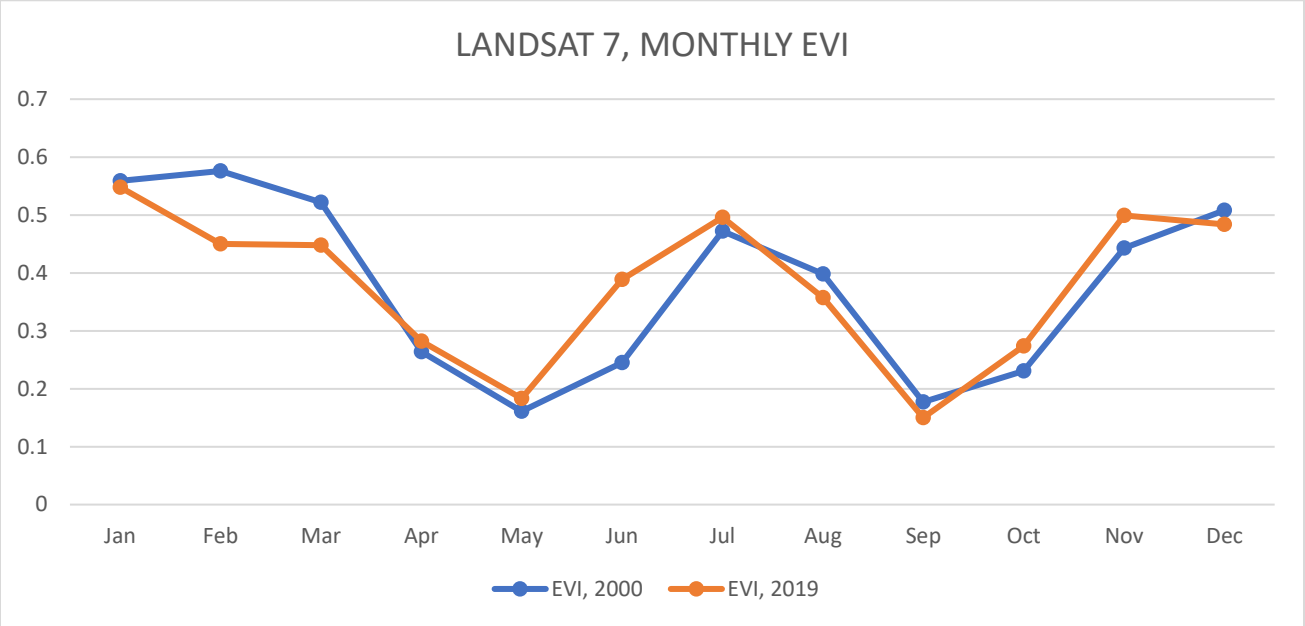

Figure 3.16 Landsat 7, monthly EVI, 2000 VS 2019

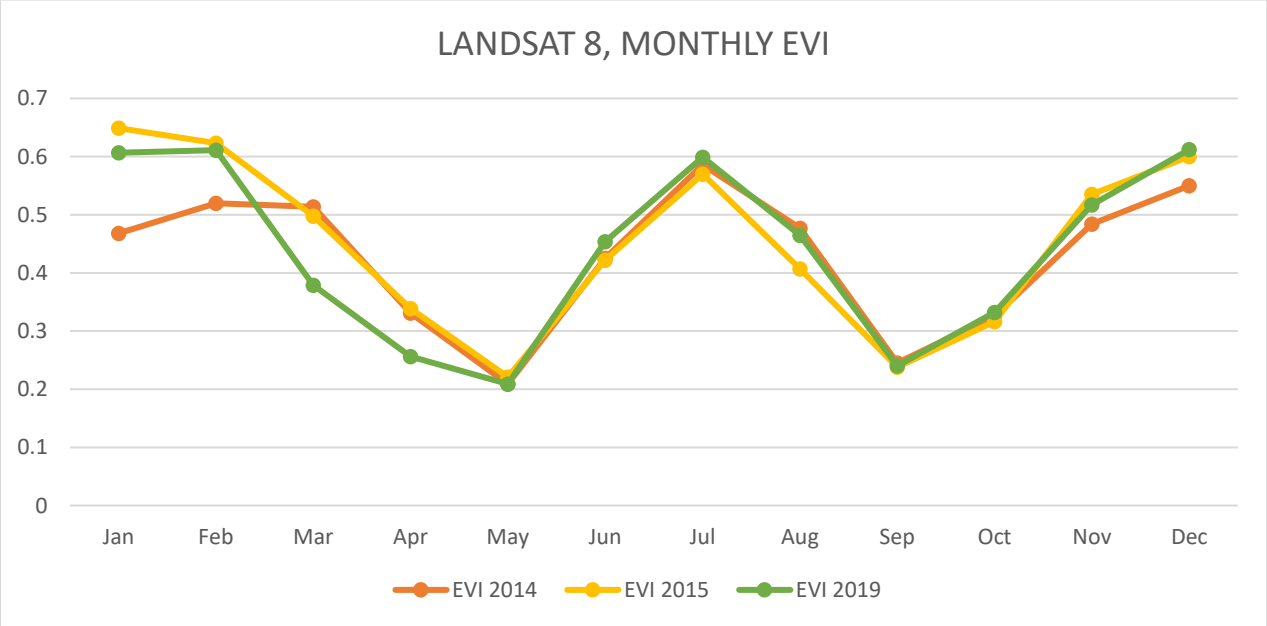

Figure 3.17 Landsat 8, monthly EVI, 2014 VS 2015 VS 2019

The results show that September and May have the minimum values over the year while January, February and July have the highest value over the year. The vegetation indices are low in September and then they are incrementally increasing until January which has the highest value over the year. After January, the vegetation indices are incrementally decreasing until May. Then, start increasing again until July. And after, the vegetation indices are decreasing until September. The results of region 2 is like region 1 since they have the same characteristics. The main reason of dividing them is the division of the River Nile in region 3 into two distributaries Rasheed and Damietta. Region 2 shows constant vegetation level over the last 20 years.

3.9 Region 3

Figure 3.18 Region 3

Region 3 is in south of Delta. It includes the capital Cairo with an area 5341 km^2. The area consists of small farms that cultivate seasonal crops as shown in Figure 3.19. The area depends on surface

water from Nile River for irrigation. Using EVI from Landsat 7, the average value of each 32 days has been calculated over the last 20 years as shown in Figure 3.20.

Figure 3.19 High resolution satellite image shows the dense cultivation system in Region 3

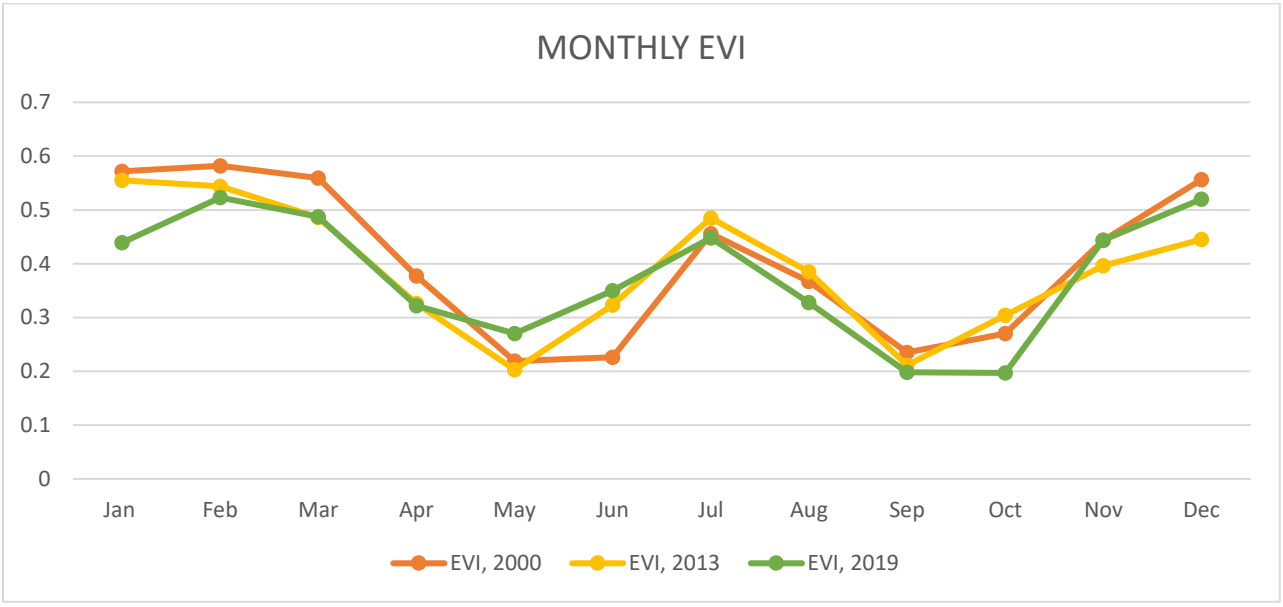

Figure 3.20 Landsat 7 EVI for 2000 VS 2013 VS 2019

The results show that the vegetation level did not change during the last 20 years. During each year, there are high values during January and February because it is a mid-agriculture season of winter. The values decrease until the harvest time in May and then, increase again until July which is the mid agriculture season of summer. After, the vegetation value decreases until the harvest time in October.

3.10 Region 4

Figure 3.21 Region 4

Region 4 is in west of Delta with an area 4584 km^2. This area is depending on both surface water and underground water for irrigation. And, it consists of farms that cultivate seasonal crops and trees as shown in Figure 3.22. The distribution over each year and the average annual value over last 20 years has been calculated as shown in Figure 3.23 and 3.24.

Figure 3.22 High resolution satellite image shows the presence of trees in Region 4

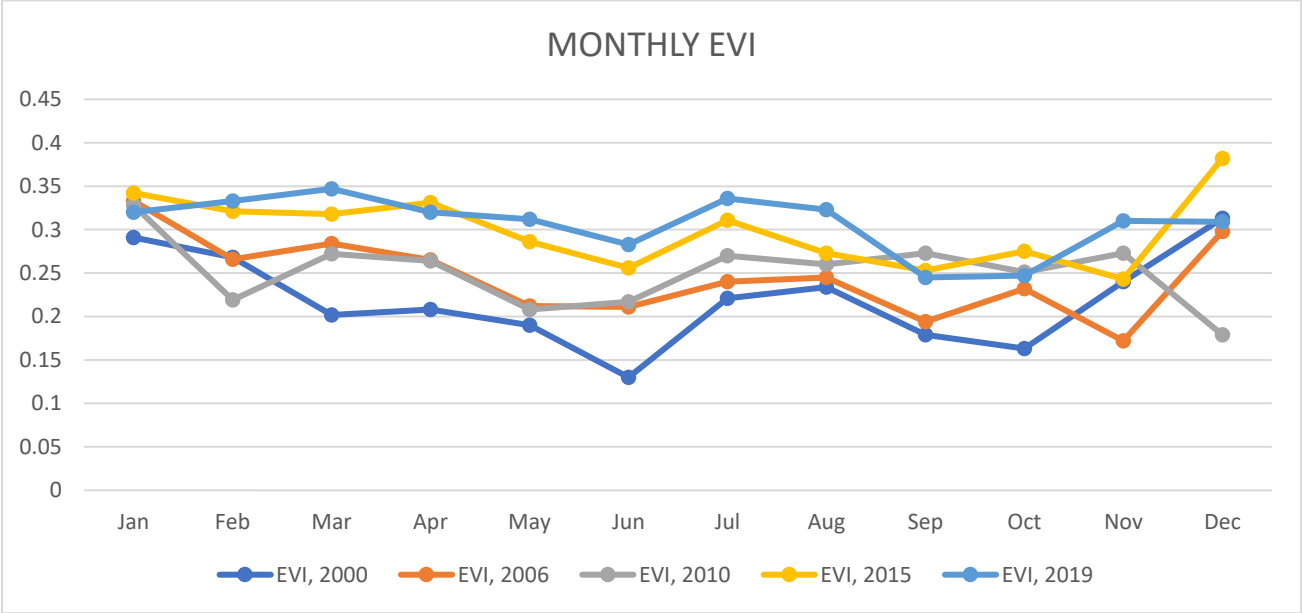

Figure 3.23 Landsat 7 EVI for 2000 VS 2006 VS 2010 VS 2015 VS 2019

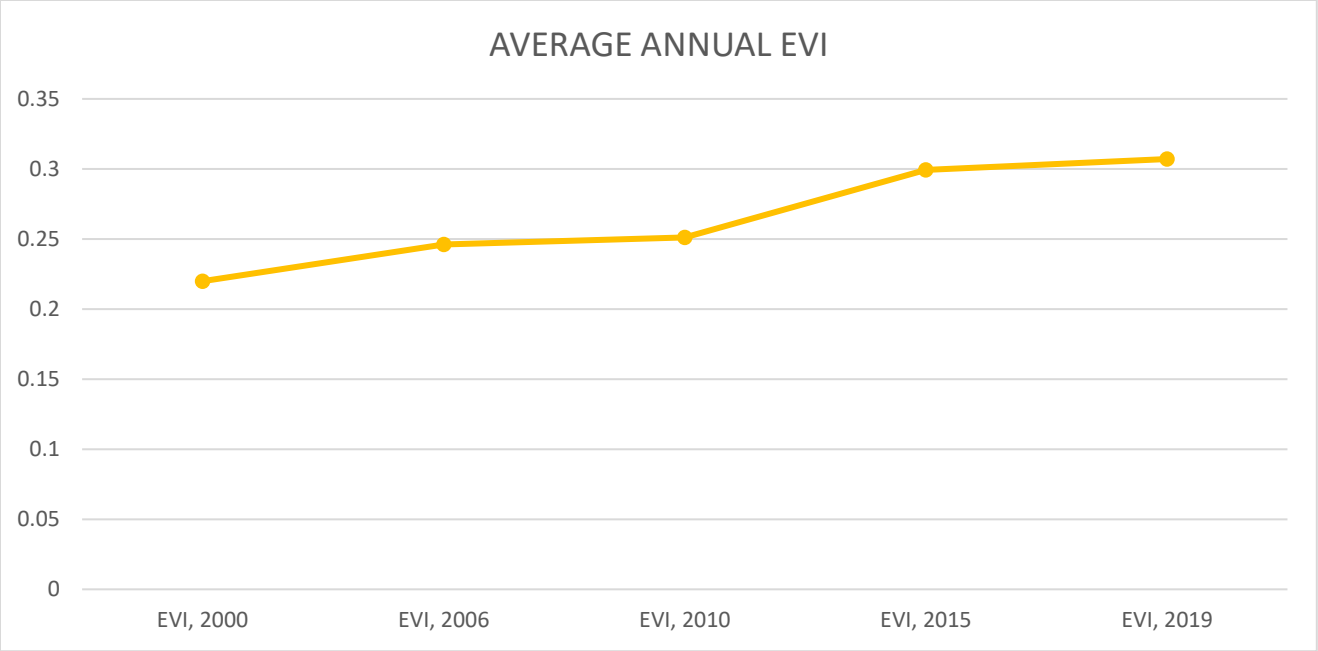

Figure 3.24 Landsat 7, Average annual EVI for 2000, 2006, 2010, 2015, 219

The results of Figure 3.24 show that the vegetation index increased between 2000 and 2019. This increase is due to reclamation of new lands that depend only on underground water. The results of Figure 3.23 show that the monthly distribution of vegetation level is more homogeneous comparing to region 1, 2 and 3 because it has high percent of trees which provide constant level of vegetation over the year, unlike crops which provide seasonal greenness.

3.11 Region 5

Figure 3.25 Region 5

Region 5 is west of Delta close to west desert with an area 4119 km^2. This area depends on underground water for irrigation. It consists of farms that cultivate trees and crops. This area uses developed irrigation system as pivot system, drop system and spray system as shown in Figure 3.26.

Figure 3.26 High resolution satellite image shows the presence of Pivots in Region 5

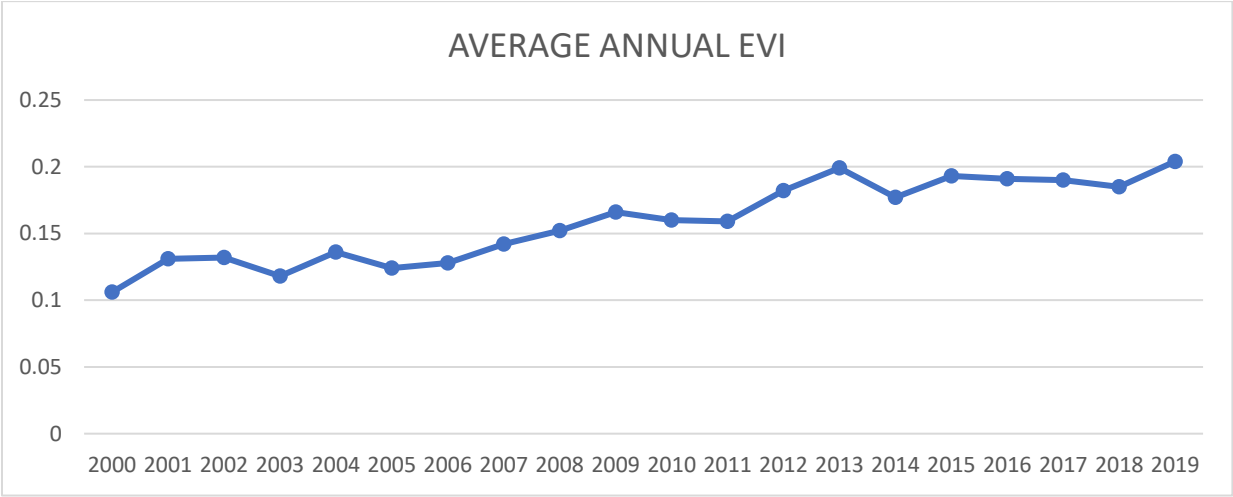

Figure 3.27 Landsat 7 average annual EVI over last 20 years

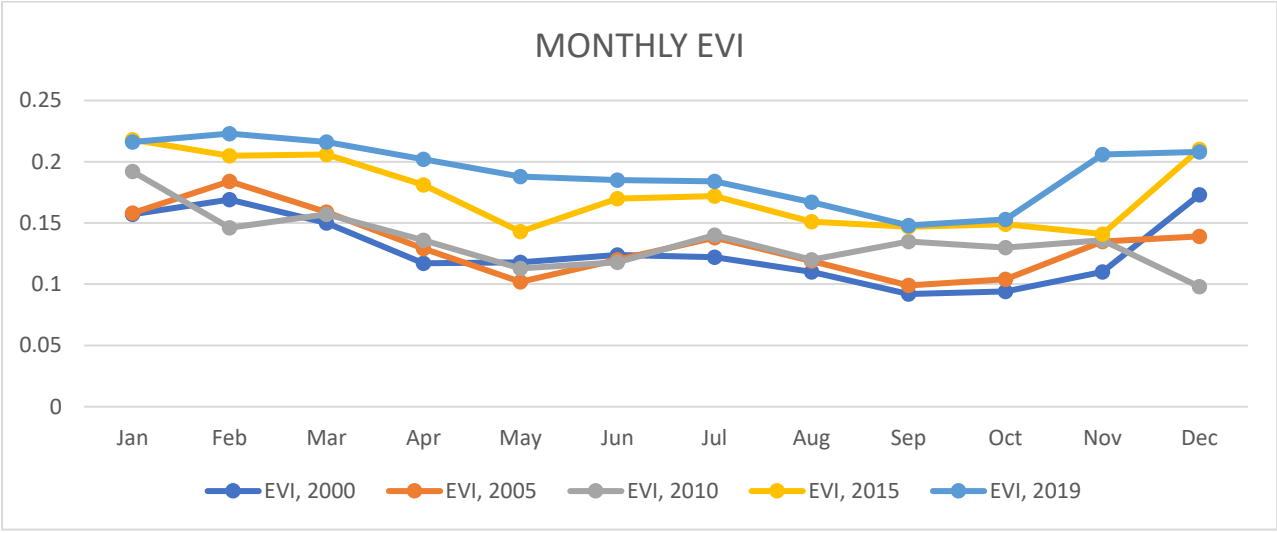

Figure 3.28 Landsat 7, monthly EVI for 2000 VS 2005 VS 2010 VS 2015 VS 2019

The results show that there is significant increase in vegetation level during the last 20 years as shown in Figure 3.27 and 3.28. The reason behind vegetation level increasing is the reclamation of new lands depending on underground water and developed irrigation system like pivot and drop system. The average vegetation index still less than the mid of delta region because there are a lot of infiltrated areas didn't reclaim yet. Region 5 considered extension of Delta region toward desert and it is west of Alexandria-Cairo Desert Road.

3.12 Region 6

Figure 3.29 Region 6

Region 6 is east of Delta close to east desert with an area 5225 km^2. This area is the east extension of Delta Region. This area depends mainly on underground water for irrigation except small areas which depend on surface water. Many farms in this area are using pivot irrigation system as shown in Figure 3.30. The average annual EVI has been calculated over the last 20 years as shown in Figure 3.31.

Figure 3.30 High resolution satellite image shows the presence of pivots in Region 6.

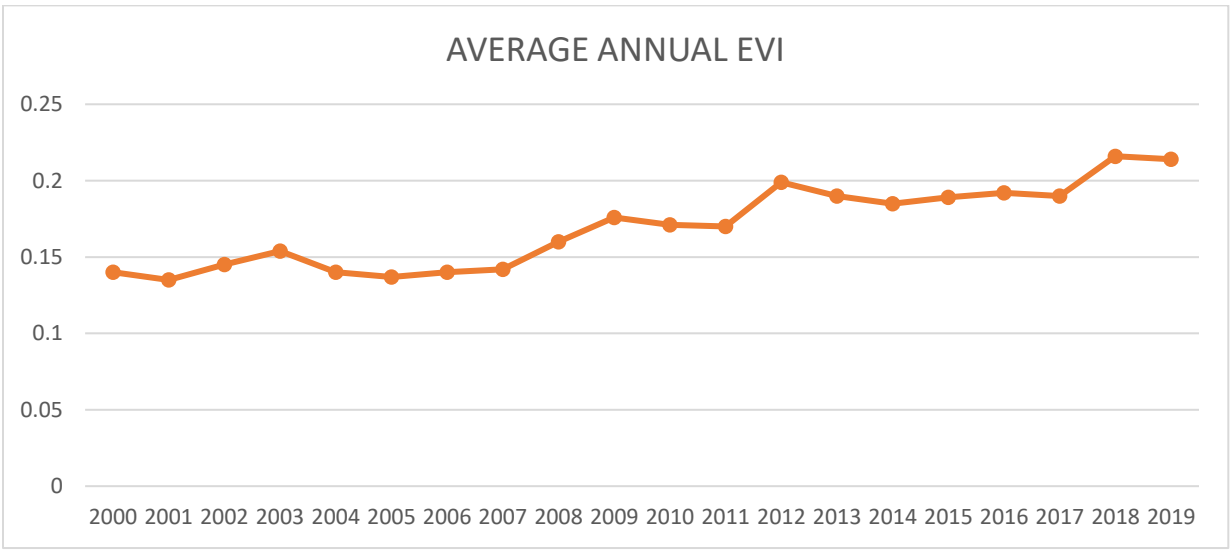

Figure 3.31 Landsat 7, average annual EVI over last 20 years

The results show that there is incremental increase of vegetation level during last 20 years due to the expansion of using underground water. Still the average vegetation level is less than mid of delta because there are infiltrated desert areas.

3.13 Summary of the results

The results show that region 1, 2 and 3 have high vegetation level that is due to the availability of surface water from the Nile river, infrastructures for water supply and services in Delta region. While, going far from Delta the vegetation level goes down. Region 4, 5 and 6 have lower vegetation level due to the lack of water, the high cost of using underground water, the high cost of pivot and drop system and the lack of infrastructures and services (FAO, 2007). Region 4 depend on both surface water and underground water so, the vegetation level increased during the last 20 years. Region 5 and 6 depend mainly on underground so, the vegetation level increased during last 20 years but still the vegetation level is less than surface water dependant areas due to the limitation of using underground water. Using underground water has many limitations such as needing source of energy like electricity or diesel to bring up the water from underground. In some areas, the underground water is 200 m under the ground surface and in some other areas it is deeper than 200 m. Due to not having infrastructures and source of electricity, some farms are using diesel for the water pump which has a lot of malfunctions and high cost. Most of the farmers that used diesel pump have complained the scarcity of diesel during crises times and some of them give up and stopped their projects. Also, Considering the storage limitation of underground water and water pumping high cost, underground water dependant areas need to use high cost developed irrigation systems such as pivot and drop system to reduce water consumption. The developed irrigation system is expensive comparing to irrigation by immersion. Both water pump and developed irrigation system need regular maintenance, have malfunctions and extra cost for the farmers. Despite of all these limitations, the vegetation level is increasing on the underground water dependant areas because that is one of the little alternatives to cover the shortage of surface water and the high demand of food.

Using the vegetation indices is very effective tool to measure the change on the ground but the characteristics of the region need to be considered. Different from some studies that linked vegetation index in Egypt with availability of Nile river water, Vegetation level increase for Region 5 and 6 is independent on Nile river water. The increase of vegetation level in region 5 and 6 may cover part from expected vegetation level reduction in region 1, 2 and 3 dues to GERD.

Region 1, 2 and 3 did not affected yet because the Egypt share of Nile water has reduced the Naser lake storage. When Naser lake storage finish, Vegetation reduction of regions 1, 2 and 3 is expected.

Chapter 4: Developing WebGIS Application through Earth-Engine to show the Impact of GERD on Egypt

4.1 Background about Web Geographic Information Systems (WebGIS)

Figure 4.1 Transformation of GIS data (ersi.com, 2020)

In the last years, the distribution of spatial and non-spatial data on the internet plays a crucial role in facilitating communication based on data between administration, decision-makers and citizens. In order to encourage the sharing and disseminating of Geographic data, Web Geographic Information Systems (WebGIS) was developed. WebGIS (also known as web-based GIS and Internet GIS) denotes a type of Geographic Information System (GIS), whose client is implemented in a Web browser. WebGIS is web-based application that allows sharing GIS through internet. Web-GISs have been developed and used extensively in Earth-Observation applications. WebGIS is connecting A common task for GIS and web applications to make services available to others within and outside the organization of the data provider. A WebGIS can provide different capabilities to users such as reading data, editing data, or producing analysis. Also, it allows users to work on the same project in the same time from different places. Furthermore, users can review the progress of other's work, which offer possibilities to access the right data in the right time to make the right decisions. In general, WebGISs are not as complex for users like GIS software such as ArcView, ArcInfo, or MapInfo, so WebGIS usually doesn't require a powerful computer or extensive training and there are also opensource applications which do not require any license to be used.

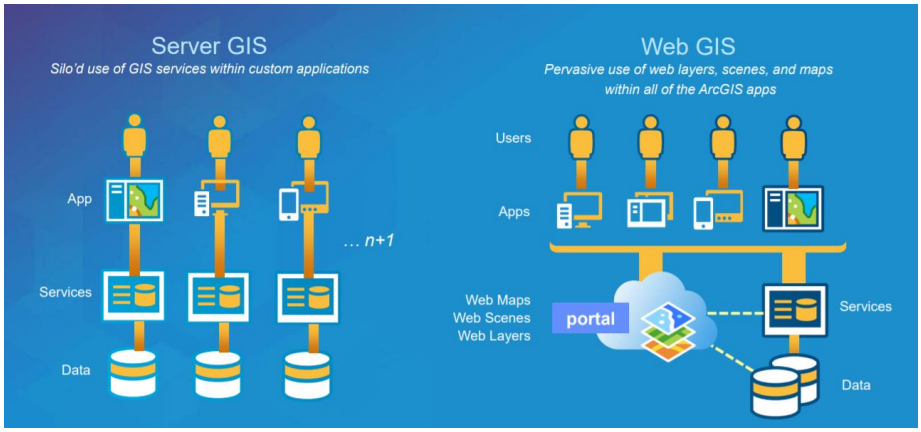

Figure 4.2 Difference between Server GIS VS WebGISIS (ersi.com, 2020)

4.2 WebGIS Architecture

A WebGIS centres around one or more machines called servers that respond to requests from other machines, called clients. Servers are usually configured with more computing power than clients and run specialized operations in response to client requests. They may also send data to clients for processing. GIS-focused servers can perform cartography and spatial processing operations such as drawing maps and running geo-computational algorithms, respectively (Peng, 1999).

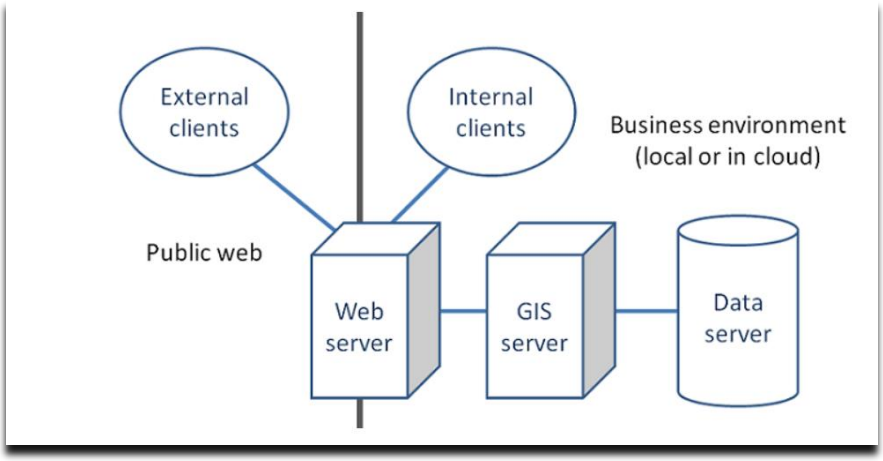

Figure 4.3 Elements of a common WebGISIS architecture (gistbok.ucgis.org, 2020).

4.3 Earth Engine Applications characteristics

Earth Engine Apps are dynamic, shareable user interfaces for Earth Engine analyses. With Apps, experts can use simple user interface (UI) elements to leverage Earth Engine's data catalogue and analytical power, for experts and non-experts alike to use. Apps published from Earth Engine are

accessible from the application-specific URL generated at time of publishing. No Earth Engine account is required to view or interact with a published App. Apps selected as featured by their creator are also available at a user-specific App Gallery. Earth Engine Apps can take advantage of most of the same functions used in the Code Editor, with some exceptions and advantages. Earth Engine provides access to client-side user interface (UI) widgets through the UI package. These interfaces can include simple input widgets like buttons and checkboxes, more complex widgets like charts and maps, panels to control the layout of the UI, and event handlers for interactions between UI widgets.

4.4 Developing WebGIS Application by Earth Engine for showing Impact on Agriculture in Egypt

In this thesis, two WebGIS Applications have been created using Earth Engine in order to develop easy fast tools for measuring GERD impact on Egypt. The first Application draws annual EVI chart for the period between 2013 until now over different provinces of Egypt. The application has been created to observe vegetation level changes during the past and is ready to do it for the following years. In fact, the vegetation area extension is expected to decrease in the next few years due to water shortage in Egypt as a consequence of GERD filling. The second application draws monthly EVI chart for 2019 and displays five maps of Min EVI, Max EVI, average EVI, average precipitation and average evaporation during 2019. The second application has been created to observe monthly changes in vegetation level and other important factors affecting agriculture in Egypt during 2019. Both applications have been designed to be used by either advanced or basic GIS knowledge users. Furthermore, the applications highlight the impact of GERD on water storage in Egypt.

4.5 EVI profile tool Application

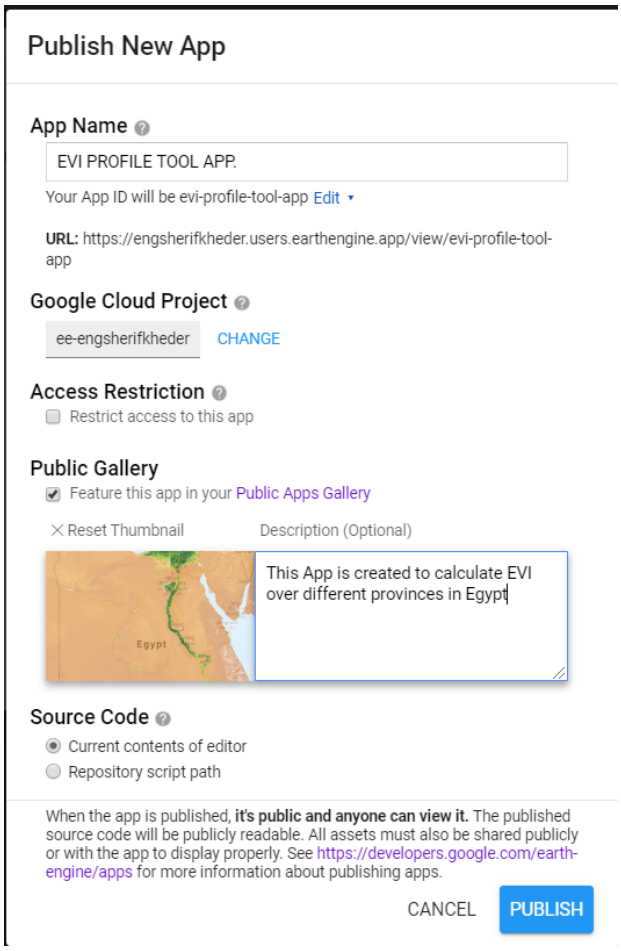

Figure 4.4 EVI Profile tool publishing features.

The application could be published either for specified users or in public. So that they could view, interact, modify, or save the application on their account. This application has been published in the public gallery to be available for anyone. The application is accessible using any web browser through the application generated URL. As all the processing procedures are performed on Earth Engine processor the application does not require hight performance processor and could be accessible from simple devices. Moreover, Earth Engine users could view, update, modify the application without changing the URL, however users are not authorized to modify the application source code.

4.5.1 Application structure and data catalogue

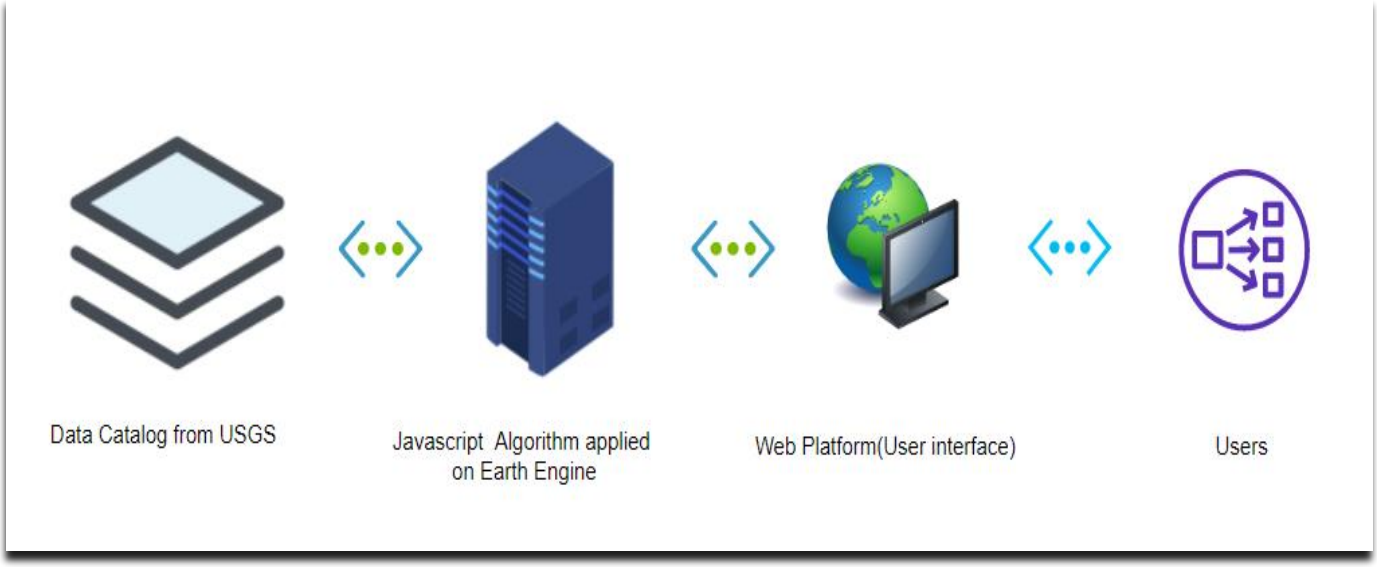

Figure 4.5 The structure of WebGIS Application

The application is connecting the data catalogue of USGS by using JavaScript code that is applied on earth engine. The application has limited google cloud memory to store the data from USGS, however it is possible to extend the memory by purchasing additional google cloud storage. The memory extension would increase the capability of the application to serve more users. Moreover, the earth engine processes the application using a mega computer consequently, reducing both processing cost and time for the users.

4.5.2 Application algorithm

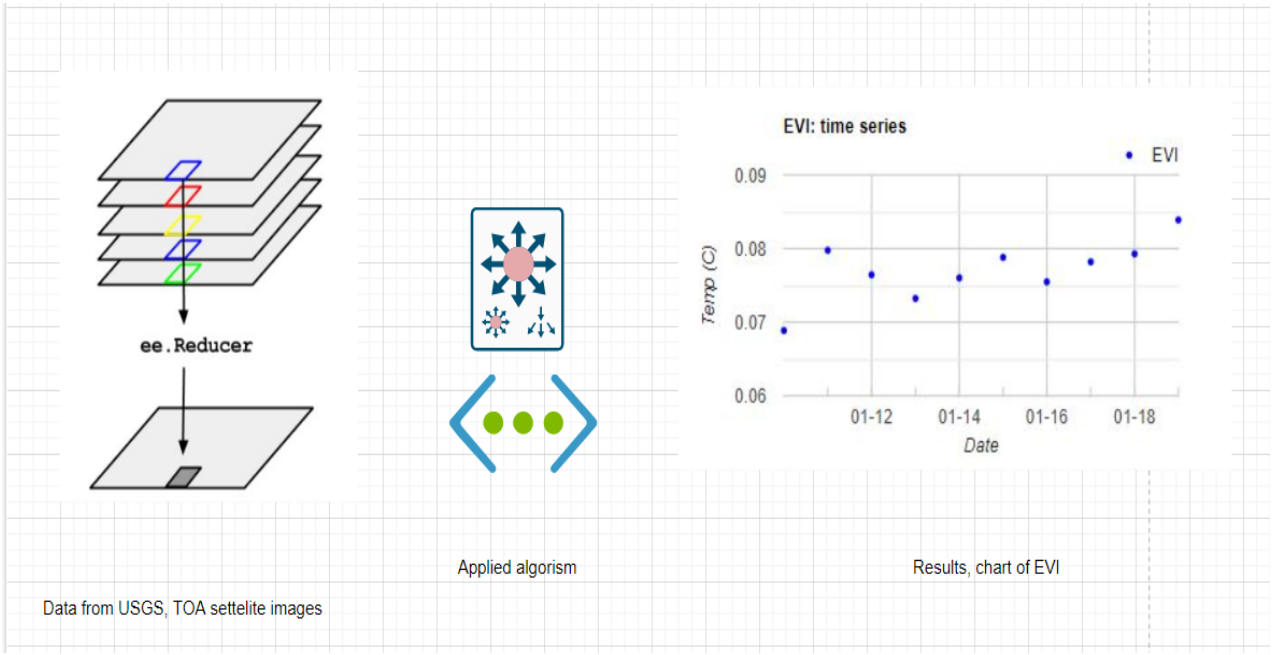

Figure 4.6 The algorism process starting from the row images to the results

The application algorithm has been developed using JavaScript programming language and applied on Earth Engine. The main function of the algorithm is to display a chart of EVI over the last 7 years for a preselected province in Egypt. The algorithm inputs are the satellite images that have been collected from USGS and its output is EVI annual chart for a province which can be selected by the user. There are one TOA satellite image every 16 days and 24 satellite images per year. The processing phase is divided into three steps. In the first step, the TOA satellite images are clipped to have the same boundary of the corresponding province. In the second step, the average annual EVI is calculated from clipped TOA images. Third step, all the results are collected in the final chart.

4.5.3 Platform interface

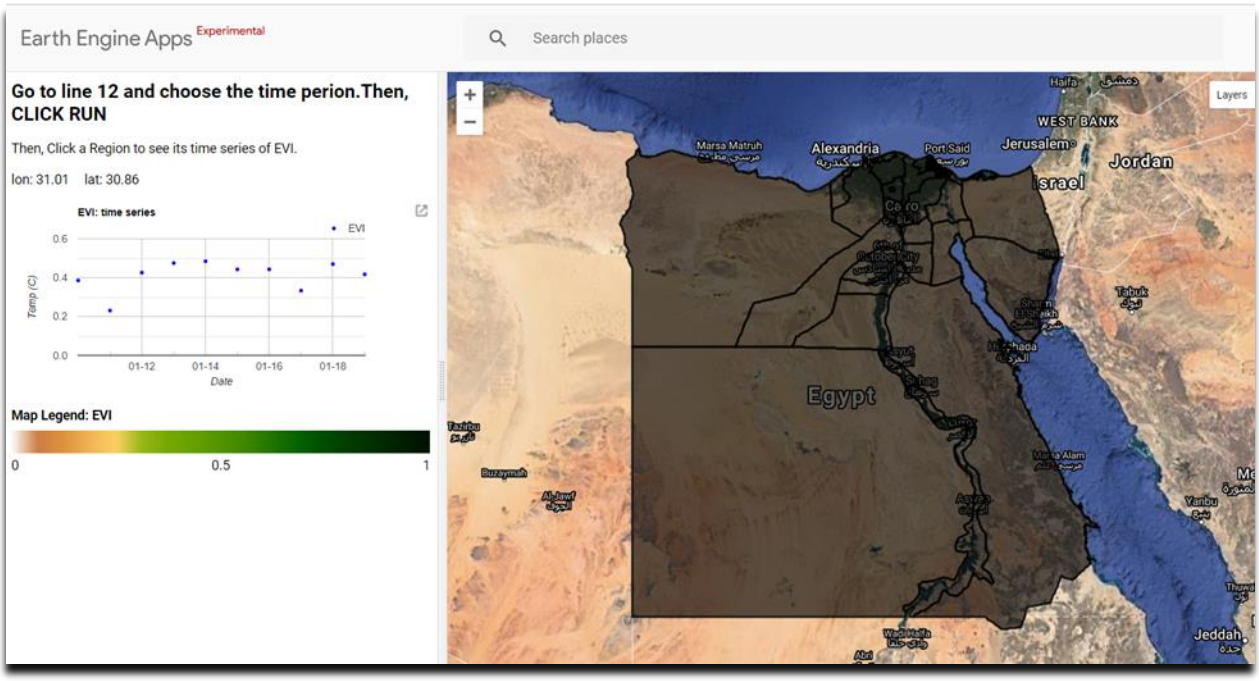

Figure 4.7 User Interface of EVI profile tool Application

https://engsherifkheder.users.earthengine.app/view/app-final2

The EVI profile tool application could be accessed through the above URL. This platform interface is divided into two sub panels: layers panel and chart panel. The layers panel is designed to hold two layers; one for the Egyptian provinces map, and the other for selected point. The layer panel divided the map of Egypt into 27 provinces. The chart panel provides the user with chart, legend and instructions. When the user clicks on a point, a small circle appears on the Layers panel in that location. The coordinates of the selected point are registered, then, the corresponding province is indicated for further processing to produce the final chart. The EVI chart is implemented with respect to time (yearly). When the user clicks on another point the new coordinates are registered and the previous coordinates are deleted. Then, all the procedures can be repeated, and new chart is produced. The script of all the procedures including Input data and used functions and analysis procedures can be accessed through the link of the code editor:

https://code.earthengine.google.com/?scriptPath=users%2Fengsherifkheder%2Fcherif%3AAPP%20FINAL2

which can be accessed through regular browser. Using Code Editor, users within the same organization and external parties can review, correct, modify, or comment the analysis. Also, it is

possible for people within the same organization to work in the same project in the same time or reviewing the progress of the work. This way of sharing data is great improvement in comparison to tradition way which need sending heavy data that need to be stored on a large memory.

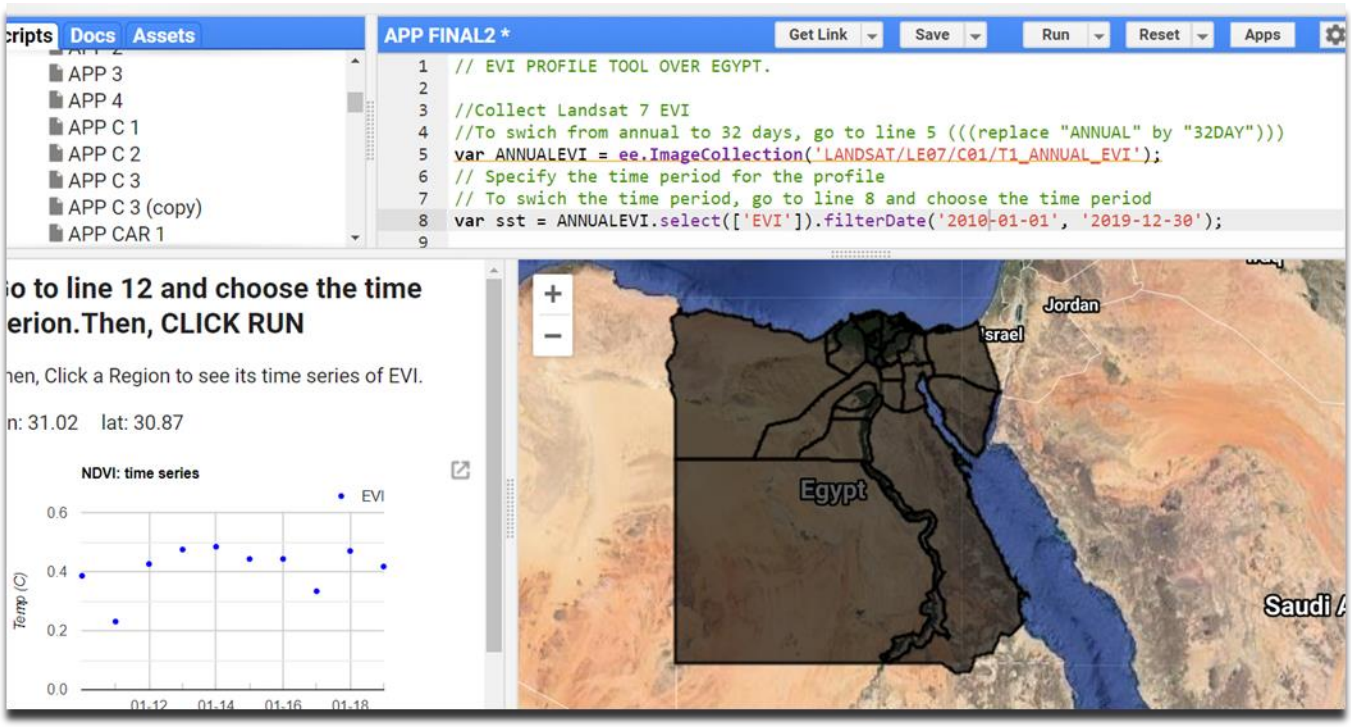

Figure 4.8 Code Editor Window of EVI profile tool

4.5.4 EVI Monthly Profile Tool and Web Map Application

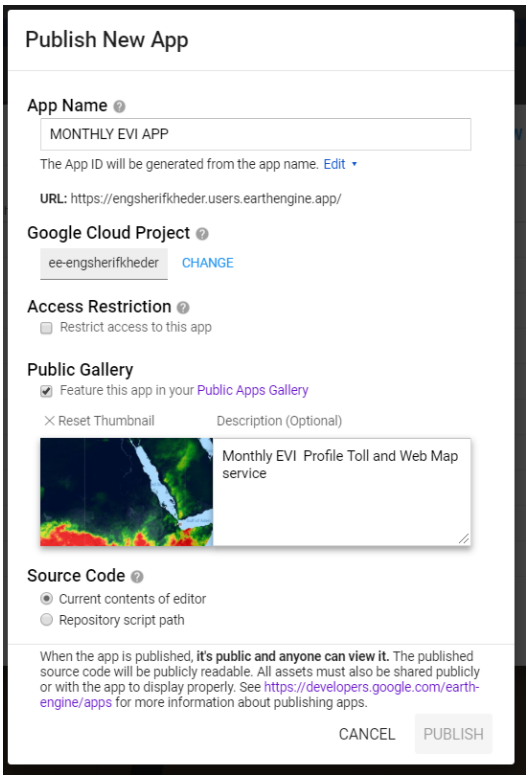

Figure 4.9 EVI Profile tool and Web map service publishing data

The application draws monthly EVI chart for 2019 and displays five maps of Min EVI, Max EVI, average EVI, average precipitation and average evaporation during 2019.While the application focuses on 2019 it could be modified by the beginning of 2021 to display different parameters for 2020. The application is public, and users have access to its source code. The application covers the whole area of Africa so, it covers Nile River upstream and downstream.

4.5.5 Application Inputs and data catalogue

The application is connected to data catalogue of USGS to obtain top of atmospheric satellite images taken by Landsat 8. In addition, the application connected to the actual evapotranspiration and interception obtained by the Food and Agriculture Organization of the United Nations (FAO,2020), and connected to precipitation map obtained by Climate Hazards Group InfraRed Precipitation (CHIRPS) (Funk, 2020). Google cloud memory is used to store the data from USGS, FAO and Climate Hazards Group while processing, so, the users do not require memory for processing.

4.5.6 Application algorithm for the Web Map application

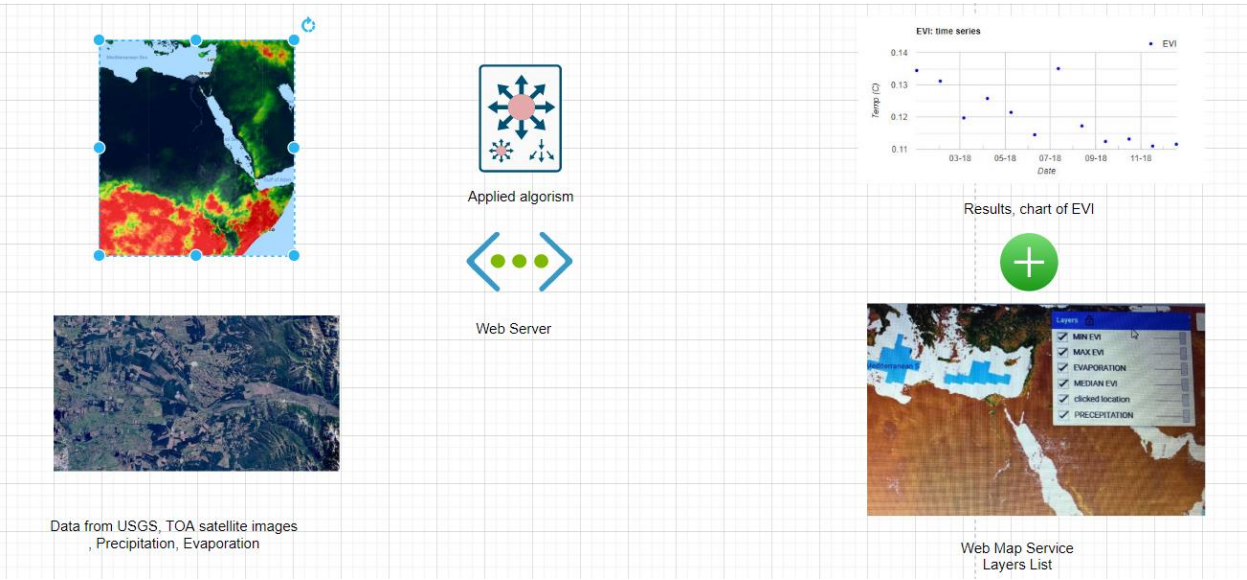

Figure 4.9 The algorism process starting from the row images to the web map service

The algorithm input are the satellite images that are called while processing from different sources. The main function of the algorithm is to display chart of monthly EVI over 2019 and to create layers panel to hold five maps, Min EVI, Max EVI, average EVI, average Evaporation, average Precipitation. First the monthly average values of EVI are calculated then, the values are filtered to get the min and max EVI values and their corresponding dates. Then, the EVI maps for the defined dates are added to the layers panel. Also, the average EVI map is calculated to be displayed in another layer. In addition, the average Precipitation of 2019 has been calculated from 72 satellite images of climate Hazards Group InfraRed Precipitation and it has been added to the layers panel. Furthermore, the precipitation provided by The Food and Agriculture Organization of the United Nations (FAO) has been added to the layers panel.

4.5.7 Platform interface for the Web Map application

The interface has been designed to show the Map panel on the right and the EVI chart on the lift. The Map panel contain layers list on the top right which includes five layers as shown in Figure 4.10. The map panel give the option to choose which layer to display. Also, it gives the option to control the transparency of the layers so two or more layers could be reviewed together. The interface could be access by any browser. The resulting chart could be opened in a separate panel and its results could be downloaded in different formats such as ee.chart, CSV or PNJ. Each layer represents important factor related to water management in Egypt.

URL: https://engsherifkheder.users.earthengine.app/view/appth-6

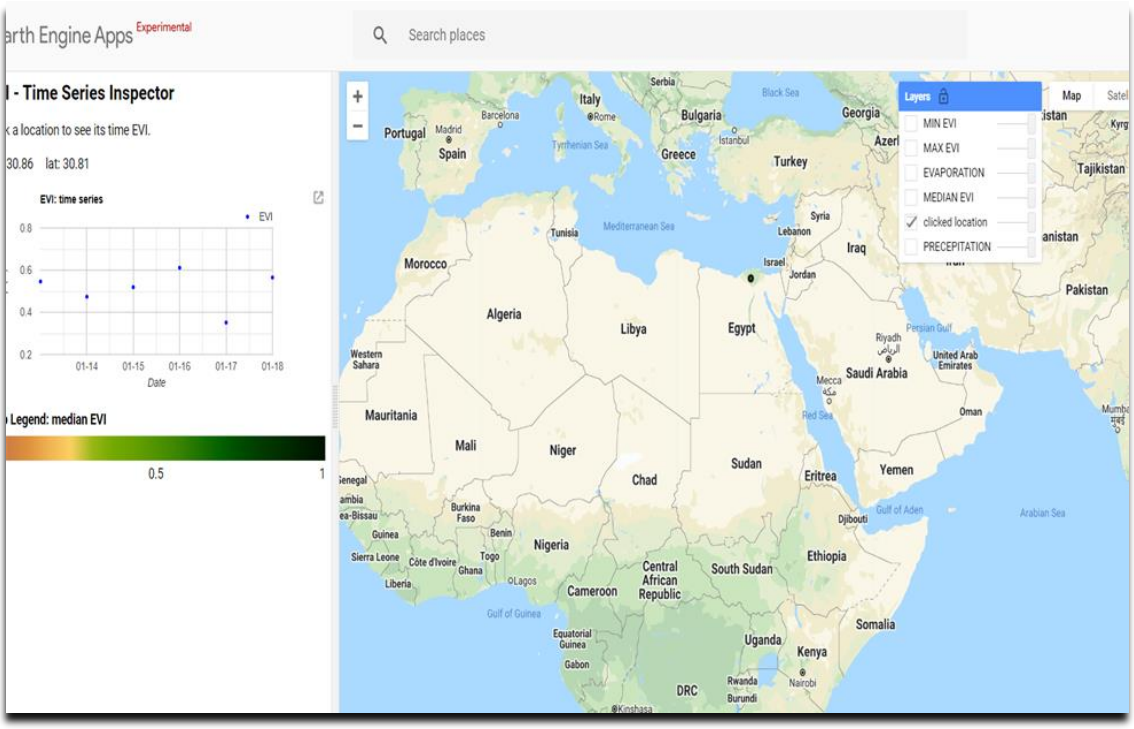

Figure 4.10 User Interface of EVI profile tool and map Application

4.5.8 The Layers of Map Panel

First layer (Min EVI) is representing the EVI map at MAY 2019. This date has the lowest EVI average over Egypt during 2019. It is important to show this map because there is significant reduction in vegetation level comparing to the rest of the year. This reduction is due to harvest time as explained in the third chapter. The area in the west do not have the same reduction rate due to the presence of high percentage of trees farms that provide constant greenness level all over the year comparing to crops farms that provide seasonal greenness.

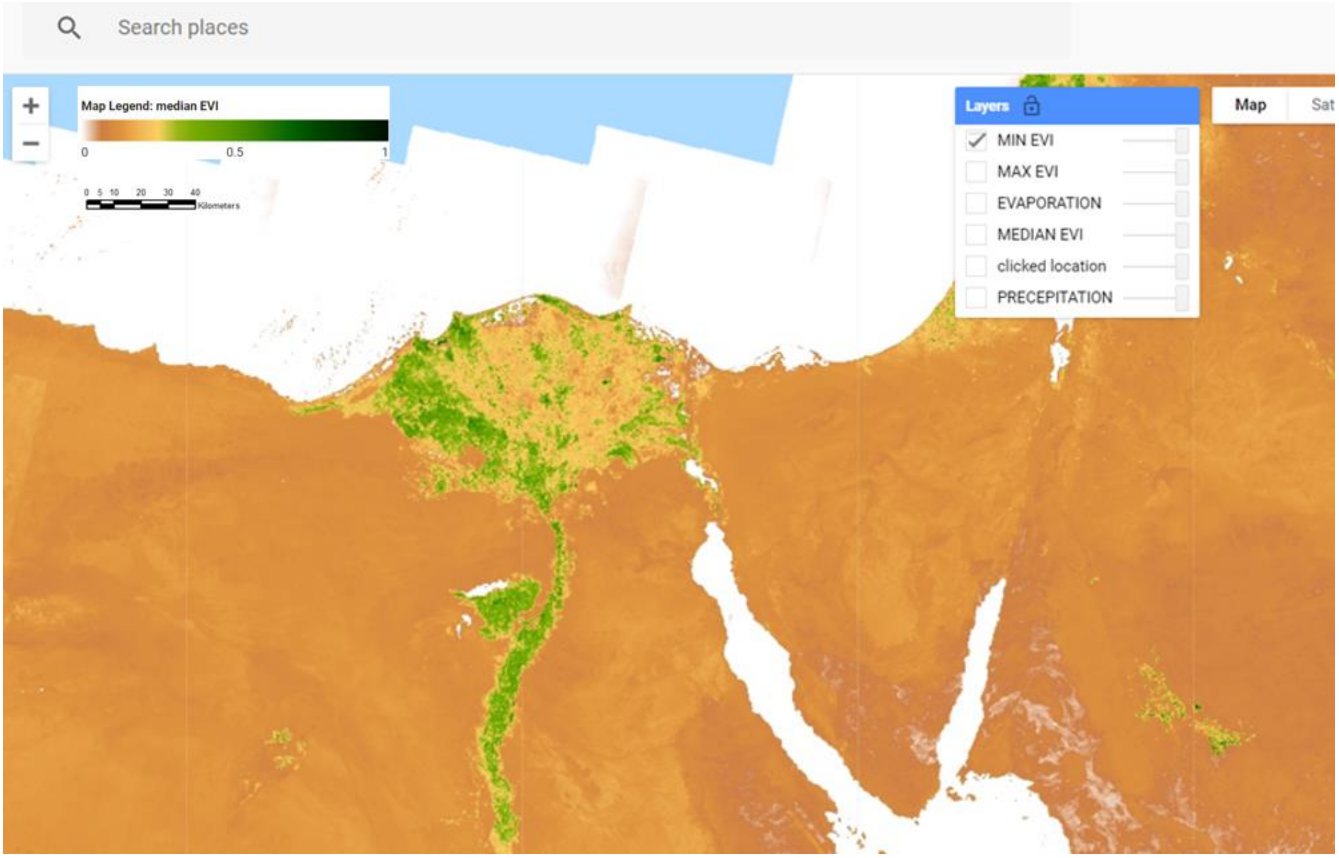

Figure 4.11 Min EVI over 2019

Second layer (Max EVI) represents the peak average value during January 2019. In this time of the year, the vegetation level goes to the maximum because it is the mid of agricultural season as explained in the third chapter. Comparing the Min EVI map with the Max EVI map, it is noticeable that the areas with high variation is depending on seasonal agriculture. While, the area with minor variation is depending on trees which provide homogenous level of vegetation all over the year. It is mostly the area on the west which has high percentage of trees farm as explained in the third chapter.

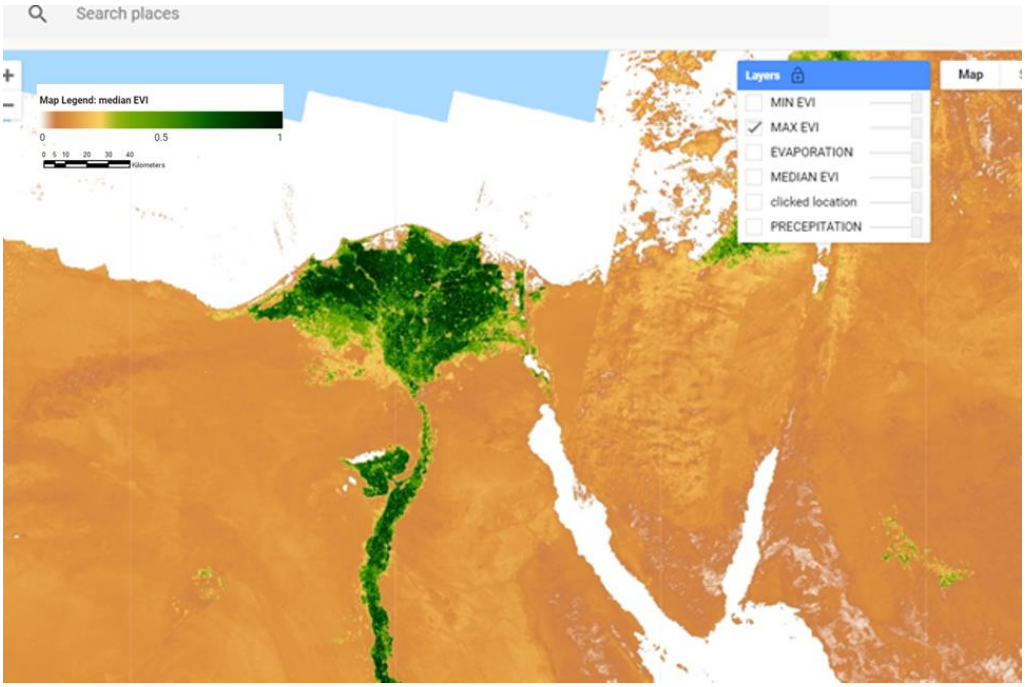

Figure 4.12 Max EVI over 2019

Third layer (Median EVI) represent the average value of EVI over 2019. It is recommended when comparing EVI between different year in the presence of seasonal agriculture to use the average because it considers 24 time points during the year. So, this layer is provided to compare the vegetation level of 2019 with other years.

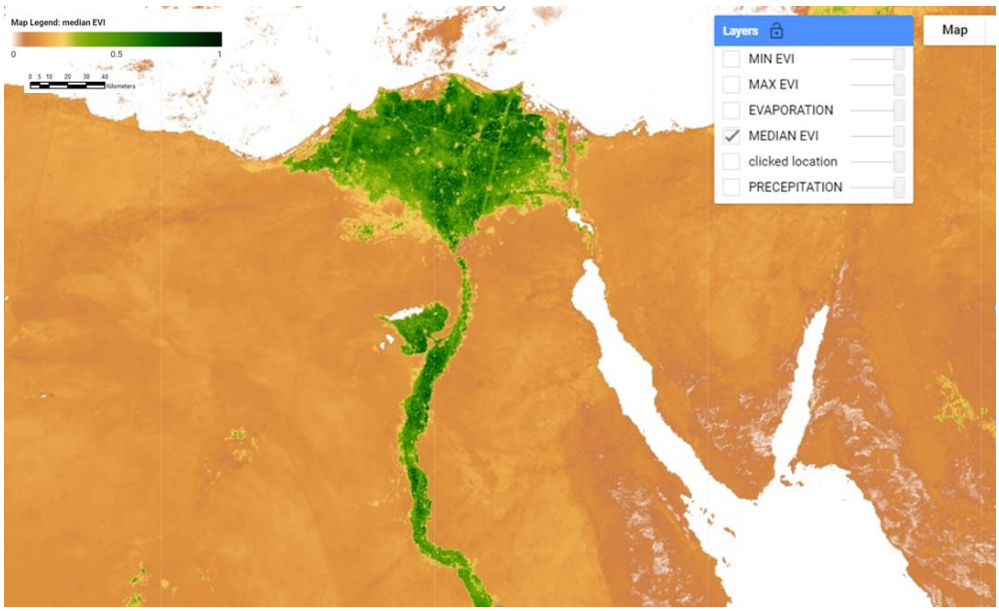

Figure 4.13 Median EVI over 2019

Fourth layer (Precipitation) has been developed on the level of Africa to show the precipitation distribution over Africa. The used unit is mm/pentad, the min value is zero and the max value equal to 1072. This map is the average precipitation over 2019. It shows that Egypt has very little rainfall and the sources of water are concentrated in south of Africa.

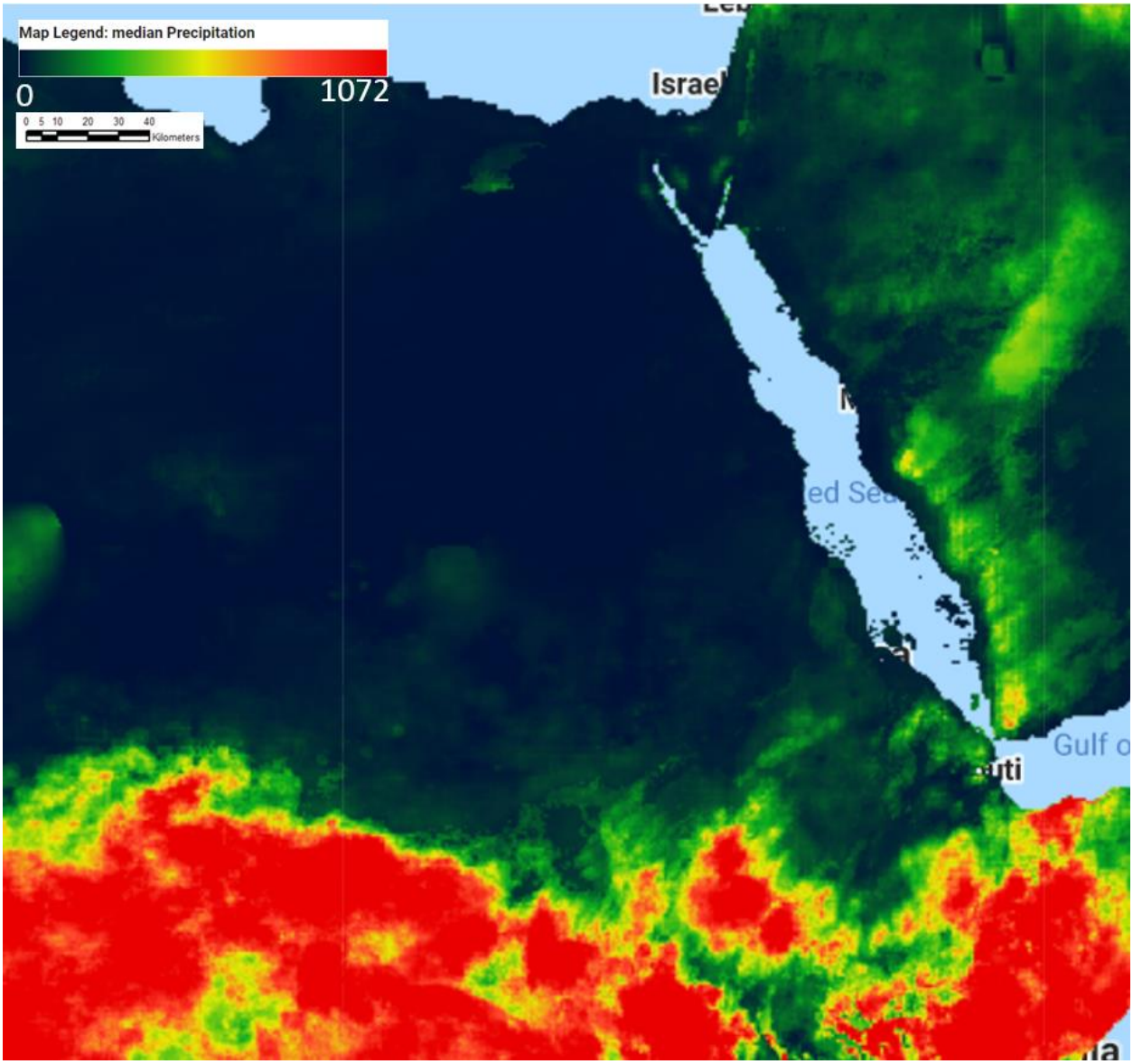

Figure 4.14 average precipitation over 2019

Fifth Layer (Evaporation) is showing the average annual evaporation of 2019. The actual evapotranspiration and interception (dekadal, in mm/day) is the sum of the soil evaporation (E), canopy transpiration (T), and evaporation from rainfall intercepted by leaves (I). The value of each pixel represents the average daily ETI in 2019.The minimum value is zero and the maximum value

is 0.1. this map has been produced by The Food and Agriculture Organization of the United Nations (FAO). FAO is mandated to collect, analyse, interpret, and disseminate information related to nutrition, food, and agriculture. In this regard, it publishes several databases on topics related to FAO's mandate, and encourages the use of them for scientific and research purposes. Consistent with the principles of openness and sharing envisioned under the Open Data Licensing for Statistical Databases.

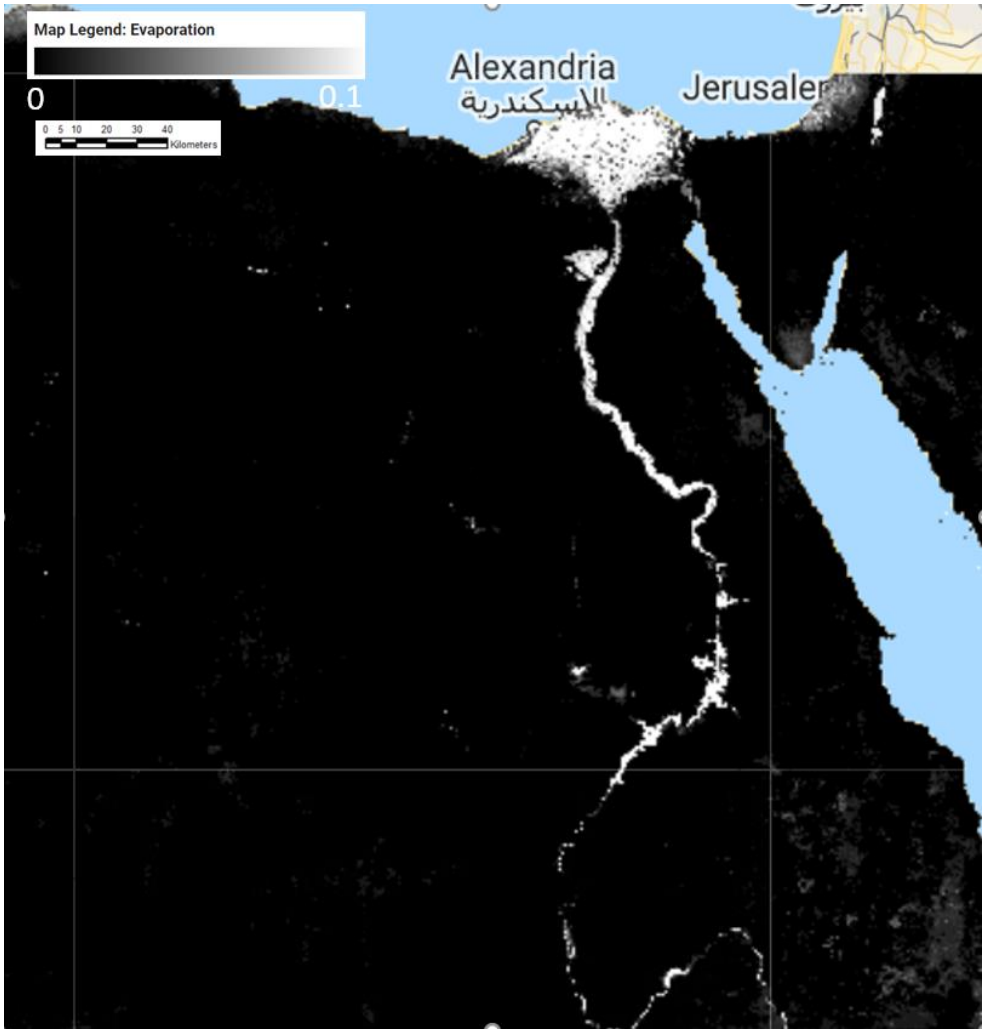

Figure 4.15 Evaporation Map(FAO,2020).

Conclusion

Ethiopia begun the construction of Grand Ethiopian Renaissance Dam (GERD) on the Blue Nile River to facilitate local and regional growth. The GERD, located just upstream of the border with Sudan, is the first dam ever to be constructed directly on the main stem of the Blue Nile and will become the largest dam in Africa. The filling of the dam will have clear implications on downstream flows in Sudan and Egypt, complicated by evaporative losses, climate variability, and climate change. In this thesis, remote sensing has been used to measure the impact of GERD on the downstream country, Egypt. Web Geographic information application is created through Earth Engine to produce effective tool for measuring the consequent vegetation changes. The application is calculating Enhanced Vegetation Index (EVI) for different regions downstream during past 20 years. It has been developed to assess the effects of the dam on agriculture in Egypt specially Delta region, which considered the last region before the Nile River mouth. Also, the developed application is dynamic shareable interface that can be used either by experts or non-experts. Moreover, organizations can collaborate through the created application to overcome communication challenges during crises or disasters events. In other hand, most agriculture in Egypt depends on Nile River Water Except new reclaimed areas that depend on underground water and it represents less than 10% of water consumption in Egypt. The results show that the mid of Delta Region vegetation level decreased at very low rate during the last 10 years due to the extension of urban area over agricultural area. Nevertheless, the mid of Delta still has high vegetation level because of the availability of surface water from the Nile river, infrastructures for water supply and available services in the region. Furthermore, the vegetation level in the east and west Delta, which depend on underground water, gradually increased during the last 20 years. Instead, the vegetation level in the east and west of Delta is lower than the middle of Delta (surface water dependant area) due to the limitation of underground water use. The use of vegetation indices represents a very effective tool to measure vegetation variation, but the characteristics of the region need to be considered as well. In general, the growth of natural forest is proportional to rain fall intensity. However, the agriculture growth in the mid of Delta, and the west of Delta are proportional to the surface water and underground water, respectively. Furthermore, dependency on underground water for irrigation is decreasing the storage of underground water. Also, evaluating agricultural areas through vegetation indices need to consider agriculture seasonal variation because in harvest time there is a significant decrease while in the mid of the season there

is a peak so, choosing determined time point is a key factor for reasonable monitoring. Comparing Enhanced Vegetation Index (EVI) with Normalized Vegetation Index (NDVI), it has been found that EVI is more sensitive to cultivation vitality measuring and its trend is closer to describe cultivation seasonal change.

References

Yengoh, G., Dent, D., Olsson, L., & Tengberg, A. (2015). Use of the Normalized Difference Vegetation Index (NDVI) to Assess Land Degradation at Multiple Scales. *SPRINGER BRIEFS IN ENVIRONMENTAL SCIENCE*.

Ahmed , A., & Ahmed , U. (2008). Sediment in the Nile River system. In UNESCO-IHPInternational. UNESCO-IHPInternational.

Arjoon, D., Mohamed, Y., Goor, Q., & Tilmant, A. (2014). Hydro-economic risk assessment in the eastern Nile River basin. *Water Resources and Economics*.

Bank, W. (2006). *Managing water resources to maximize sustainable growth: A Country water resources assistance strategy for Ethiopia.* Washington, DC.

Bates, A., Tuncok, K., & Barbour, T. (2013). *First joint multipurpose program identification: Strategic perspectives and options assessment on the Blue Nile multipurpose development* . Addis Ababa: Author Report to Nile Basin Initiative.

Block, P., & Rajagopalan, B. (2009). Statistical-dynamical approach for streamflow modeling at Malakal, Sudan, on the White Nile river. *J. Hydrol. Eng., 10.1061/(ASCE)1084-0699(2009)14:2(185),* , 185–196.

Block, P., & Strzepek, K. (2010). Economic analysis of large-scale upstream river basin development on the Blue Nile in Ethiopia considering transient conditions, climate variability, and climate change. *Journal of Water Resources Planning and Management*.

Brown, C., Lund, J., & Cai, X. (2015). The future of water resources systems analysis: Toward a scientific framework for sustainable water management. *Water Resources Research*.

Cartney, M., & Girma, M. (2012). Evaluating the downstream implications of planned water resource development in the Ethiopian portion of the Blue Nile River. In *Water International* (pp. 362–379).

Conway, D. (2000). The climate and hydrology of the upper blue Nile,Ethiopia. *Geog. J., 166(1),*, 49–62.

Dandan, X., & Xulin, G. (2014). Compare NDVI Extracted from Landsat 8 Imagery with that from Landsat 7 Imagery. *researchgate*.

EarhEngine. (www.earthengine.com). *https://cloud.google.com/storage/docs/public-datasets/landsat*.

EDF, & Scott Wilson. (2007). *Eastern Nile power trade program study: Pre-feasibility study of border hydropower project, Ethiopia.* Addis Ababa: Author report to Nile Basin Initiative.

El-Nashar, W., & Elyamany, A. (2017). Managing risks of the Grand Ethiopian Renaissance Dam on Egypt. *Ain Shams Eng J.*

Elsahabi MA, M., & Negm , A. (2016). Performances evaluation of surface water areas extraction techniques using Landsat ETM+ Data: case study Aswan High Dam Lake (AHDL). Proc Technol.

ersi.com. (2020). *proceedings.esri.com*. Retrieved from ersi.com.

FAO. (2007).

FAO. (2018). *Level 1. Remote Sensing for Water Productivity Technical Report: Methodology Series. Rome, FAO. 72 pages.* WaPOR Database Methodology.

Funk. (2020). *The climate hazards infrared precipitation with stations—a new environmental record for monitoring extremes.*

gistbok.ucgis.org. (2020). *gistbok.ucgis.org*.

Group of Nile Basin, C. (2013). *Egyptian Chronicles: Cairo University's report on Ethiopia's Great Renaissance Dam*. Retrieved from http://egyptianchronicles.blogspot.co.uk/2013/06/cairouniversitys

Guariso, G., & Whittington, D. (1987). Implications of ethiopian water development for Egypt and Sudan. *International Journal of Water Resources Development*.

Hassan, A. (2012). *Eastern Nile Planning Model (ENPM) project: Water balance model for the Eastern Nile Basin. Dhaka.* Author report to Nile Basin Initiative.

https://earthengine.google.com/. (n.d.). Retrieved from EarthEngine: https://earthengine.google.com/

Huete , A., Kidman, K., Miura, T., Rodriguez, E., Goa, X., & Ferriera, L. (2002). Overview of the radiometric and biophysical performance of the MODIS vegetation indices. *Remote Sensing of Environment*.

Ibrahim, A. (2017). Impact of Ethiopian Renaissance Dam and Population on Future Egypt Water Needs. *American Journal of Engineering Research (AJER)* .

IDSC . (2007). *(Information and Decision Support Center).* Cabinet of Ministers, Egypt.

Jensen, J. (2007). Remote sensing of the environment. Pearson Prentice Hall. *Upper Saddle River*.

Jeuland, M. (2010). Economic implications of climate change for infrastructure planning in transboundary water systems: An example from the Blue Nile. *Water Resources Research*.

Jeuland, M., & Whittington, D. (2014). Water resources planning under climate change: Assessing the robustness of real options for the Blue Nile. *Water Resources Research*.

King, A., & Block, P. (2014). An assessment of reservoir filling policies for the Grand Ethiopian Renaissance Dam. *Journal of Water and Climate Change*.

Liersch, S., & Koch , H. (n.d.). *Management scenarios of the Grand Ethiopian Renaissance Dam and their impacts under recent and future climates.* Retrieved from Water 9(728).

Mohamed, N. (2017). Journey from Origin to End. *Springer International Publishing*.

Mulat, A., & Moges, S. (2014). Assessment of the impact of the Grand Ethiopian Renaissance Dam on the performance of the High Aswan Dam. *Journal of Water Resource and Protection*.

NBI. (2012). *Nile Basin Initiative.* Retrieved from State of the River Nile Basin. : http://nileis.nilebasin.org/

Nevin. (2019). *A WebGIS prototype to show the impact of the Grand Ethiopian Renaissance Dam on Egypt fresh water availability*.

Nigatu , G., & Dinar , A. (2015). Economic and hydrological impacts of the Grand Ethiopian Renaissance Dam on the Eastern Nile River Basin. In *Environ Dev Econ 21* (pp. 532–555).

NWRP. (2004). *National Water Resources Plan (NWRP).* National Water Resources Plan (NWRP).

Peng. (1999). Retrieved from https://gistbok.ucgis.org/.

Post-Gazette, W. w. (2014). Retrieved from http://www.PittsburghPost-Gazette.com.

Rouse , J., Haas , R., & Schell , J. (1977). *Monitoring vegetation systems in the Great Plains with ERTS.* NASA Spec.

Salman, S. (2013). The Nile basin cooperative framework agreement : A peacefully unfolding African spring? *Water Int., 38(1)*, 17–29.

Sharaki , A. (2013). The Ethiopian Renaissance Dam: development and policy considerations. *Center for the Development of Natural and Human Resources in Africa,Cairo University*.

Sutcliffe, J., & Parks, Y. (1987). Hydrologic modeling of the Sudd and Jongeli cana. *J. Hydrol. Sci., 32(2),* , 143–159.

Tayie, M. S. (2018). *The Grand Ethiopian Renaissance Dam and the Ethiopian Challenge of Hydropolitical Hegemony on the Nile Basin.* Cairo: Springer, Cham.

The Open Geospatial Consortium (OGC). (n.d.). Retrieved from www.ogc.org.

Tucker, C., & Garratt , M. (1977). Leaf optical system modeled as a stochastic process. In *Appl Optics.*

UNEP/MAP Regional Activity Centre. (2011). *Water use efficiency and economic, National study Egypt.*

visual-paradigm.com. (2020). Retrieved from https://www.visual-paradigm.com.

Wagdy, A. (2010). An overview of Groundwater Management in Egypt. *Journal of Engineering and Applied Sciences. Faculty of Engineering, Cairo University* .

Wagdy, A. (2010). An overview of Groundwater Management in Egypt. *Journal of Engineering and Applied Sciences. Faculty of Engineering, Cairo University*.

Wheeler, K., & Setzer, S. (2012). *Eastern Nile RiverWare planning model.* Addis Ababa: Author report to Nile Basin Initiative.

www.smartdraw.com. (2020). *www.smartdraw.com*.

www.vineview.com. (2019).

Yao, H., & Georgakakos, A. (2003). The Nile decision support tool, river simulation and management. *Atlanta: Georgia Institute of Technology*.

Yates, D., & Strzepek, K. (1998). Modeling the Nile basin under climate change. *J. Hydrol. Eng., 10.1061/(ASCE)1084-0699(1998)3:2(98)*, 98–108.

Yates, D., Sieber, J., Purkey, D., & Huber-Lee, A. (2005). A demand-, priority-, and preference-driven water planning model. *Water International*.

Zhang , Y., Erkyihum , S., & Block , P. (2016). illing the GERD: evaluating hydroclimatic variability and impoundment strategies for Blue Nile riparian countries. In *Water Int 41:593–610.*